

RESEARCH ARTICLE

The Gene Regulatory Network of Lens Induction Is Wired through Meis-Dependent Shadow Enhancers of *Pax6*

Barbora Antosova^{1,2}, Jana Smolikova¹, Lucie Klimova¹, Jitka Lachova², Michaela Bendova¹, Iryna Kozmikova¹, Ondrej Machon¹, Zbynek Kozmik^{1,2*}

1 Laboratory of Transcriptional Regulation, Institute of Molecular Genetics, Academy of Sciences of the Czech Republic v.v.i., Prague, Czech Republic, **2** Laboratory of Eye Biology, Institute of Molecular Genetics, Academy of Sciences of the Czech Republic v.v.i., Division BIOCEV, Prague, Czech Republic

* kozmik@img.cas.cz



CrossMark
click for updates

 OPEN ACCESS

Citation: Antosova B, Smolikova J, Klimova L, Lachova J, Bendova M, Kozmikova I, et al. (2016) The Gene Regulatory Network of Lens Induction Is Wired through Meis-Dependent Shadow Enhancers of *Pax6*. PLoS Genet 12(12): e1006441. doi:10.1371/journal.pgen.1006441

Editor: Ruth Ashery-Padan, Tel Aviv University, ISRAEL

Received: September 18, 2015

Accepted: October 21, 2016

Published: December 5, 2016

Copyright: © 2016 Antosova et al. This is an open access article distributed under the terms of the [Creative Commons Attribution License](https://creativecommons.org/licenses/by/4.0/), which permits unrestricted use, distribution, and reproduction in any medium, provided the original author and source are credited.

Data Availability Statement: All relevant data are within the paper and its Supporting Information files.

Funding: This work was supported by the Czech Science Foundation (GACR 15-23675S) to ZK, by the Grant Agency of Charles University (GAUK-16063) to BA, by the Ministry of Education, Youth and Sports (LK11214, LO1419) to OM and ZK and by institutional support from the Biotechnology and Biomedicine Centre of the Academy of Sciences and Charles University (CZ.1.05/1.1.00/02.0109). The funders had no role in study design, data

Abstract

Lens induction is a classical developmental model allowing investigation of cell specification, spatiotemporal control of gene expression, as well as how transcription factors are integrated into highly complex gene regulatory networks (GRNs). *Pax6* represents a key node in the gene regulatory network governing mammalian lens induction. Meis1 and Meis2 homeoproteins are considered as essential upstream regulators of *Pax6* during lens morphogenesis based on their interaction with the ectoderm enhancer (EE) located upstream of *Pax6* transcription start site. Despite this generally accepted regulatory pathway, Meis1-, Meis2- and EE-deficient mice have surprisingly mild eye phenotypes at placodal stage of lens development. Here, we show that simultaneous deletion of *Meis1* and *Meis2* in presumptive lens ectoderm results in arrested lens development in the pre-placodal stage, and neither lens placode nor lens is formed. We found that in the presumptive lens ectoderm of Meis1/Meis2 deficient embryos *Pax6* expression is absent. We demonstrate using chromatin immunoprecipitation (ChIP) that in addition to EE, Meis homeoproteins bind to a remote, ultraconserved SIMO enhancer of *Pax6*. We further show, using *in vivo* gene reporter analyses, that the lens-specific activity of SIMO enhancer is dependent on the presence of three Meis binding sites, phylogenetically conserved from man to zebrafish. Genetic ablation of EE and SIMO enhancers demonstrates their requirement for lens induction and uncovers an apparent redundancy at early stages of lens development. These findings identify a genetic requirement for Meis1 and Meis2 during the early steps of mammalian eye development. Moreover, they reveal an apparent robustness in the gene regulatory mechanism whereby two independent "shadow enhancers" maintain critical levels of a dosage-sensitive gene, *Pax6*, during lens induction.

Author Summary

While significant insights into the functional role of some transcription factors during lens formation have been accomplished, much less is known about the intricate wiring of

collection and analysis, decision to publish, or preparation of the manuscript.

Competing Interests: The authors have declared that no competing interests exist.

the gene regulatory network (GRN) that controls the earliest stages of lens development. Our genetic experiments presented here demonstrate a fundamental and redundant role of *Meis1* and *Meis2* genes in the process of lens induction. Furthermore, we present evidence that the robustness and dose-dependent regulation of *Pax6*, a key node of lens GRN, occurs via employment of "shadow enhancers" powered by Meis transcription factors. Combined, this study significantly extends knowledge about the genetic wiring of the earliest stages of eye development.

Introduction

Cellular and molecular mechanisms of vertebrate lens development are objects of intense studies for many decades, reviewed in [1]. In particular, lens induction represents a classical developmental model allowing investigation of cell specification, spatiotemporal control of gene expression, as well as the integration of signaling pathways and transcription factors into highly complex gene regulatory network (GRN). At the end of neural plate formation, the vertebrate lens originates from the multipotent pre-placodal ectoderm [2, 3] through a series of cell-type specifications, governed by DNA-binding transcription factors Pax6, Six3 and Sox2, and including another transitional population of cells, the presumptive lens ectoderm (PLE). The PLE gives rise to the lens placode, readily observed as a thickening of the head surface ectoderm (SE) that is in close contact with the underlying optic vesicle, an evaginating part of the future diencephalon. Genetic dissection of lens induction has mainly focused on the function of Pax6, Six3 and Sox2, coupled with studies of BMP, retinoic acid and Wnt signaling in the surface ectoderm, neuroectoderm, and surrounding periocular mesenchyme, reviewed in [1]. *Pax6*-deficient (*Pax6*^{Sey/Sey}) mice are anophthalmic with eye development arrested at the optic vesicle stage [4–6]. Numerous studies have shown that Pax6 is essential for lens formation through its expression in the SE and PLE, and in the subsequent stages of lens placode formation [7–9]. In contrast, the role of Six3 and Sox2 are less clear, although it is known these factors play major roles in anterior forebrain development and optic cup formation [10–12], further enforcing *Pax6* as an ideal node to decipher genetic wiring of lens induction. Despite a well-established genetic role, much less is known about the factors operating upstream of *Pax6* and their interaction with cis-regulatory elements that direct *Pax6* expression to the lens ectoderm. Since lens development is sensitive to Pax6 dosage [4] accurate regulation of Pax6 expression level during lens development is therefore of great importance.

Transcriptional control of *Pax6* gene expression is very complex and different cells and tissues choose specific promoters and distal regulatory regions from an archipelago of enhancers scattered within the large *Pax6* genomic region [13, 14]. The expression of *Pax6* in lens ectoderm was initially shown to be driven by an ectoderm enhancer (EE) located approximately 4kb upstream of the *Pax6* P0 promoter [15, 16]. However, genetic studies in which EE was inactivated provided strong evidence that EE is not the only regulatory element responsible for *Pax6* expression in the lens placode [17]. Surprisingly, detectable expression of Pax6 in lens placode of EE mutants remains. In fact, the relatively small reduction of Pax6 levels in EE mutants leads to only mild lens defects (such as a lens placode of reduced thickness and a small lens pit/vesicle) that do not phenocopy Pax6 deficiency in the PLE [7, 17] raising the possibility that additional regions compensate for the loss of EE. Genetic analysis of human aniridia patients has identified a highly conserved long-range cis-regulatory element called SIMO, located 150 kb downstream of *Pax6* [18] that can also direct transgene expression to the developing lens [19, 20] suggesting a role as a tissue-specific enhancer. Mouse-human sequence

conservation around the SIMO breakpoint revealed 85% nucleotide identity over a 1400 bp fragment with 500 bp core region showing 96% identity [20]. Recently, *de novo* point mutation within the SIMO region has been identified in patient suffering aniridia. This mutation disrupts an autoregulatory *PAX6* binding site in SIMO, causing defective maintenance of *PAX6* expression [19]. Remarkably, a *Pax6* autoregulatory loop has also been described in the case of the EE [21]. While autoregulation of *Pax6* is critical for lens cell-type identity, and represents a key mechanistic property of both *Pax6* lens enhancers, such a mechanism does not address the critical issue, namely the identification of upstream regulators of *Pax6*. To date, functional interactions of *Meis1/2*, *Prep1*, *Six3*, *Sox2* and *Oct1* have only been demonstrated at the EE [22–25].

Three amino acid loop extension (TALE) homeobox genes are evolutionarily highly conserved developmental regulators present in both vertebrate and invertebrate genomes. In vertebrates, TALE homeoproteins are represented by the *Pbx* and *Meis/Prep* subfamilies. *Pbx* proteins interact with *Prep* and *Meis* through a conserved amino-terminal domain while an independent protein surfaces allow *Pbx* to form trimeric complexes with *Prep* or *Meis* and *Hox*, reviewed in [26]. *Prep* and *Meis* alone preferentially bind DNA motifs with the sequence TGACAG/A, whereas *Prep-Pbx* and *Meis-Pbx* dimers bind the sequence TGATTGACAG. In mouse and human, three *Meis* homologs (*Meis1*, *Meis2* and *Meis3*) and two homologues of *Prep* (*Prep1* and *Prep2*) have been identified. Genome-wide analysis of *Meis* and *Prep* binding sites using a ChIP-seq approach have revealed their substantial specialization as well as significant regulatory coordination between these factors [27]. Biochemical and transgenic reporter studies have implicated *Meis1* and *Meis2* in the regulation of the EE of *Pax6* [22]. In addition, binding of *Prep1* to the EE has been shown to control *Pax6* levels and the timing of *Pax6* activation in the developing lens [25]. However, *Meis1* knockout mice exhibit only a mild lens phenotype at later developmental stages [28]. As *Meis1* and *Meis2* exhibit similar expression patterns during the early stages of lens development (detailed in this study) we hypothesized that they are genetically redundant. To test this hypothesis, we have generated a *Meis2* floxed allele and subsequently investigated the effect of *Meis2* and *Meis1/Meis2* deficiency on lens development using a lens-specific deleter *Le-Cre* recombinase [7]. We provide genetic evidence that *Meis2* alone is not essential for lens development, however combined depletion of both *Meis1* and *Meis2* proteins at the early stages of lens development demonstrate that *Meis1/2* are redundantly required for lens placode formation. Chromatin immunoprecipitation and transgenic reporter studies further dissect the molecular mechanism of *Meis*-dependent regulation of *Pax6* gene expression. Deletion of SIMO region by genomic engineering *in vivo* suggests its redundancy with EE and uncovers SIMO function in lens development. Moreover, simultaneous deletion of EE and SIMO *in vivo* resulting in loss of lens formation confirms the essential role of the two *Pax6* enhancers for lens induction. Remarkably, our data demonstrate the existence of two independent and partially redundant *Meis*-dependent enhancers, with similar molecular architecture, involved in the regulation of *Pax6* expression during lens placode formation, thereby providing an unexpected level of robustness to the system.

Results

Meis1 and Meis2 are expressed in overlapping pattern throughout early lens development and are redundantly required for lens induction

In this study, we sought to determine the genetic hierarchy during early lens development by investigating the role of *Meis1* and *Meis2* homeoproteins using knockout mice. In addition, we wanted to examine the extent of *Meis*-mediated regulation of the critical eye specification

gene *Pax6* during lens induction. It was previously shown that specific deletion of *Pax6* in the PLE resulted in a failure of lens development from the lens placode stage onward [7]. The main prerequisite for transcriptional regulation of placodal *Pax6* expression by Meis proteins is their co-expression in the same tissue. Immunofluorescence using specific antibodies against Meis1 and Meis2 [22, 29, 30] revealed that both proteins were expressed in developing lens: in the PLE, lens placode and later in the lens pit (S1A–S1F Fig). Moreover the expression pattern of both Meis1 and Meis2 were overlapping with *Pax6* expression in the PLE [31].

Meis1 mutants (*Meis1*^{-/-}) do not present with arrested lens development [28]. We therefore questioned whether deletion of Meis2 may affect lens development. Accordingly, mice containing a *Meis2* floxed allele (*Meis2*^{fl/fl}) were generated (S1G Fig) and [32], and subsequently zygotic *Hprt1-Cre* mice were employed to create whole-body knockout of *Meis2* (*Meis2*^{-/-}). *Meis2*^{-/-} embryos displayed strong hemorrhage and other developmental defects and died by E14.5 [32]. However, lens development was not affected in these mutants (S2 Fig). To overcome the embryonic lethality of *Meis2* whole-body knockout and to conditionally inactivate Meis2 specifically in PLE from E9.0, *Le-Cre* mice [7], (S1H and S1I Fig) were crossed with *Meis2*^{fl/fl} mice. In *Le-Cre;Meis2*^{fl/fl} embryos Meis2 protein was efficiently deleted in the lens placode and surface ectoderm at E9.5 (S1J Fig). We accordingly analyzed lens development in the absence of Meis1, Meis2 or both factors. The morphology of lens development was examined at stages E10.0 and E12.5 on tissue sections stained with hematoxylin-eosin. As shown in Fig 1, both Meis1 and Meis2 deficient embryos developed beyond the lens placode stage and subsequently and invariantly formed a lens. Therefore, we decided to generate embryos simultaneously deficient for both Meis1 and Meis2 in PLE; *Le-Cre;Meis1*^{-/-};*Meis2*^{fl/fl} (referred thereafter as *Meis1/Meis2* double mutant). Deletion of *Meis1* and *Meis2* in the PLE of *Le-Cre;Meis1*^{-/-};*Meis2*^{fl/fl} embryos resulted in arrested lens development, characterized by a failure of the PLE to

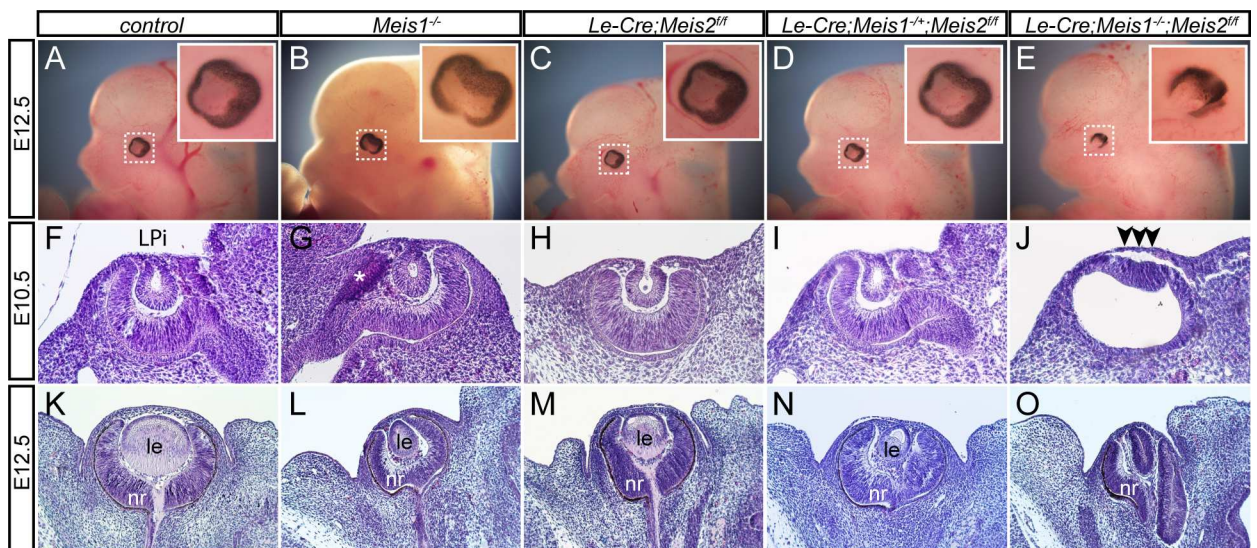


Fig 1. The phenotypic consequences of Meis1 and Meis2 deficiency. (A–E) At E12.5, external eyes of whole-mount *Meis1*^{-/-}, *Le-Cre;Meis2*^{fl/fl}, *Le-Cre;Meis1*^{-/-};*Meis2*^{fl/fl} mutant appear comparable to control eye, whereas the eye of *Le-Cre;Meis1*^{-/-};*Meis2*^{fl/fl} double mutant has abnormal shape. The insets show high magnification of eye region (boxed). (F–O) Hematoxylin-eosin stained paraffin sections show histology of control or mutant E10.5 and E12.5 eyes. (F–H, K–M) Formation of lens placode is followed by invagination of surface ectoderm, formation of lens pit (LPi) and subsequent formation of lens in control, *Meis1*^{-/-} and *Le-Cre;Meis2*^{fl/fl} embryos. (I, N) One active *Meis1* allele in *Le-Cre;Meis1*^{-/-};*Meis2*^{fl/fl} embryos is sufficient for lens placode and lens formation. (J, O) In *Le-Cre;Meis1*^{-/-};*Meis2*^{fl/fl} embryos, deficient for both Meis1 and Meis2, lens development is arrested in pre-placodal stage (arrowheads). * Artefact, le-lens, nr-neural retina.

doi:10.1371/journal.pgen.1006441.g001

thicken and form the lens placode (Fig 1). Histological analysis at E12.5 confirmed an absence of lens tissue on a morphological level in all analyzed *Meis1/Meis2* double mutants, where only folded retina was present (Fig 1O). Interestingly, one functional allele of *Meis1* in *Le-Cre; Meis1^{+/-}; Meis2^{ff}* embryos was sufficient to ensure lens placode and later lens formation, although the lenses were typically smaller (Fig 1N). These results demonstrate a requirement for Meis proteins during lens placode and subsequent lens formation.

Meis proteins are required for Pax6 expression in the presumptive lens ectoderm

To determine, whether the morphological arrest of lens development was accompanied by a loss of Pax6 expression and other lens placode markers, we performed immunofluorescent marker analyses at E10.0. Strikingly, we discovered a dramatic decrease in Pax6 expression in the PLE of *Meis1/Meis2* double mutants (Fig 2A–2B'). In addition, the expression of the lens differentiating gene *Foxe3*, which is known to be highly Pax6-sensitive [33], was also not initiated (Fig 2C–2D'). Conversely, Sox2 expression persisted in the PLE of E10.0 *Meis1/Meis2* double mutants (Fig 2E–2F'), which is consistent with Pax6-independent regulation of Sox2 at the lens placode stage [34]. Finally, Six3 expression that is mutually dependent on Pax6

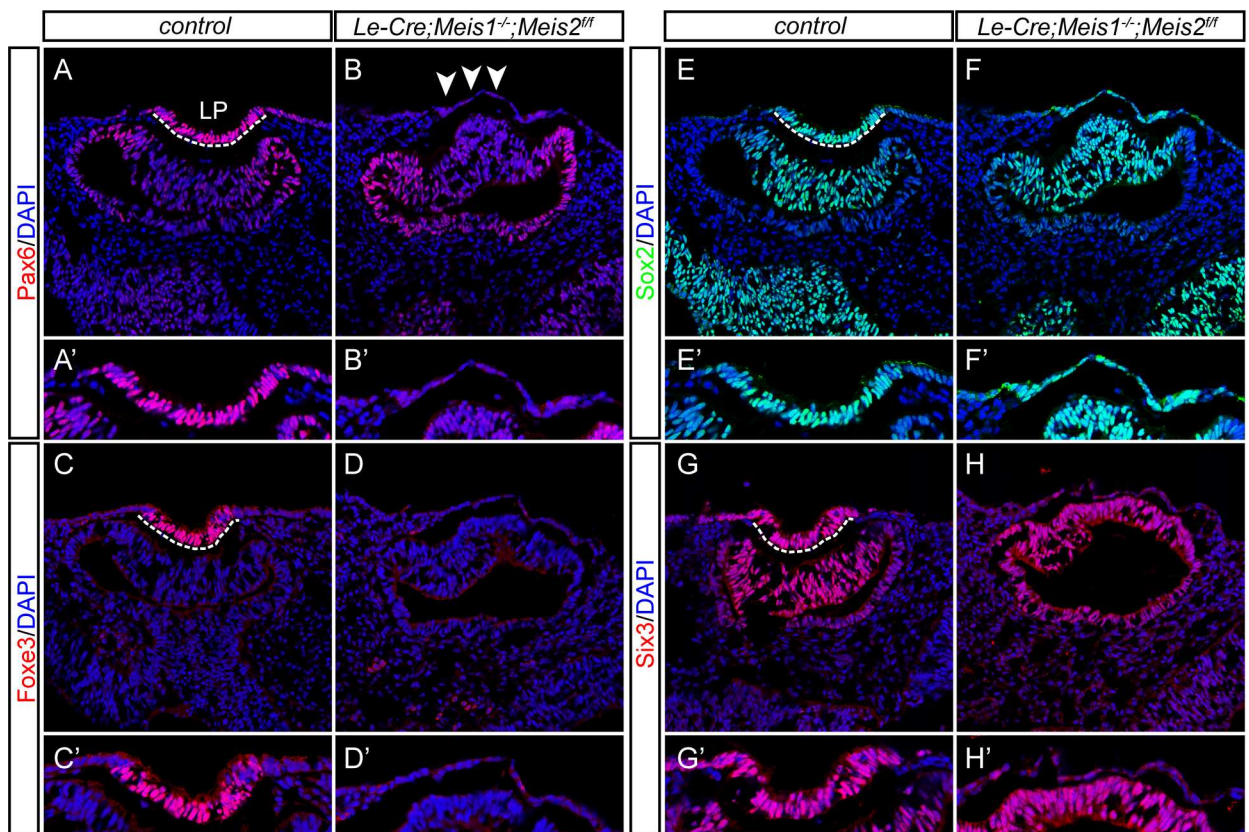


Fig 2. The expression of lens placode-specific transcription factors is disturbed in *Meis1/Meis2* double mutants. (A–H') Cryosections from E10.0 control and *Le-Cre;Meis1^{+/-};Meis2^{ff}* embryos stained with antibody as indicated and nuclei counterstained with DAPI. (B, B') Pax6 is not detected in lens surface ectoderm of *Le-Cre;Meis1^{+/-};Meis2^{ff}* embryos (arrowheads) and (D, D') expression of the lens differentiation gene *Foxe3* is not initiated. (F, F') Sox2 is detected in PLE of *Meis1/Meis2* double mutants, although it failed to thicken. (H, H') Finally, expression of Six3 is decreased compared to control. Lens placode (LP) is indicated by dashed line. (A'–H') For clearer examination, lens placode or corresponding lens surface ectoderm region is magnified and shown separately.

doi:10.1371/journal.pgen.1006441.g002

expression in the PLE [23, 35], was also decreased in *Meis1/Meis2* double mutants (Fig 2G–2H). Immunofluorescent analysis of E12.5 *Meis1/Meis2* double mutant embryos also confirmed the loss of α -crystallin-positive lens tissue, Prox1-positive differentiating lens fiber cells, Foxe3-positive lens epithelial cells and γ -crystallin-positive lens fiber cells (S3 Fig). Nevertheless, the presence of Pax6 and Sox2 proteins in the neural retina, and Otx2 in the retinal pigmented epithelium suggested that the specification of these tissues was not affected by the arrest of lens development (S3 Fig). Taken together, these results demonstrate that simultaneous inactivation of Meis1 and Meis2 results in early arrest of lens development and phenocopies Pax6 deficiency in the PLE [7].

Meis proteins bind the ultraconserved SIMO element of *Pax6* *in vivo*

A previous study has shown that Meis1 and Meis2 directly bind to the *Pax6* ectoderm enhancer (EE) and thus control Pax6 expression during early vertebrate lens induction [22]. Here we show that the simultaneous inactivation of Meis1 and Meis2 leads to the dramatic downregulation of Pax6 in PLE and arrested lens development, in a manner reminiscent of that observed in Pax6 mutants [7]. However, as deletion of the EE does not phenocopy Pax6 loss [17], we hypothesized that Meis proteins might, in addition to the EE, interact with another enhancer such as the SIMO to drive appropriate levels of Pax6 expression in the developing lens. Thus, we focused on a 1400 bp evolutionarily conserved fragment of SIMO and used chromatin immunoprecipitation (ChIP) to analyse whether Meis proteins bound the SIMO element *in vivo* (Fig 3). We initially screened the 1400 bp fragment for the presence of Meis consensus binding site sequence motif, 5' TGACAG/A 3' [36], (Fig 3B). In the most conserved core region of the SIMO, we identified five Meis binding sites named SIMO_A, SIMO_B, SIMO_C, SIMO_D, SIMO_E with SIMO_B/C/D clustered in DNA region of 77 bp (Fig 3A). As a positive control for Meis binding ChIP analyses, we used the EE as it has been previously described to be bound by Meis [22] and as negative controls, the Axin2 promoter and Neurod1 coding sequences were used. Chromatin immunoprecipitation was performed on wild-type E10.5 embryos and the α TN-4 cell line [37] representing a model of mouse lens epithelial cells. qRT-PCR analysis of DNA fragments immunoprecipitated with mixture of Meis1+Meis2 specific antibodies from in E10.5 embryos showed significant enrichment at the EE as well as at the SIMO_B/C/D putative Meis-interacting sites (Fig 3C). No enrichment was observed at the negative controls regions or at the predicted Meis binding site SIMO_A. Similar results were also obtained when α TN-4 cells were used for immunoprecipitation (Fig 3D). Taken together these data show that Meis proteins bind the SIMO element *in vivo* and suggest that simultaneous binding of both the EE and SIMO may be required for appropriate Pax6 expression in the early lens.

Reporter gene analysis indicates dominant role of Meis proteins for SIMO enhancer activity

To test the functional significance of identified Meis interactions with the SIMO enhancer we prepared reporter gene constructs expressing lacZ gene under the control of a minimal *hsp68* promoter fused to the mouse SIMO enhancer (Fig 4A and 4B). To determine the specificity of any interactions, a single point mutation was introduced into Meis binding site that changed the recognition sequence from TGACAG/A into TcACAG/A. The same G to C mutation has previously been shown to abrogate Meis binding and has been used in functional characterization of the EE and pancreatic enhancer in transgenic mouse models [22, 38]. In accordance with previous studies, FLAG-tagged Meis2 was able to specifically bind double-stranded oligonucleotides encompassing wild-type Meis binding site but not its mutated version (S4 Fig).

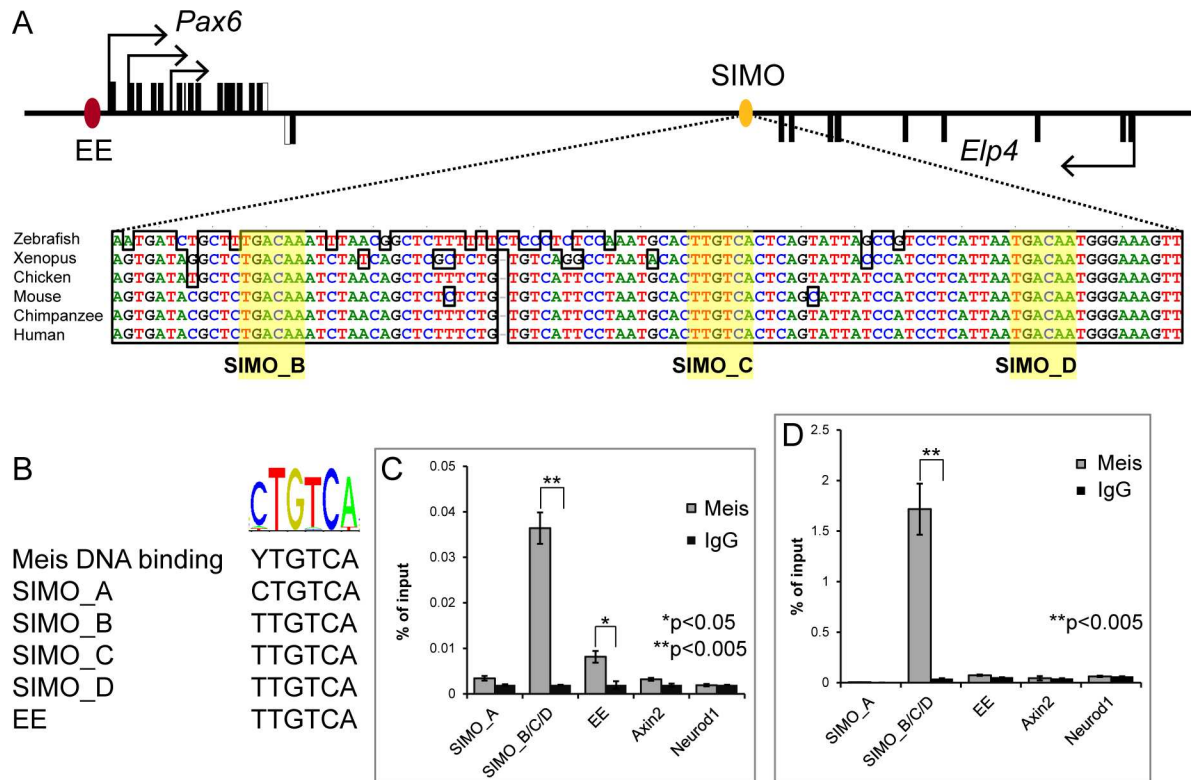


Fig 3. Meis proteins bind SIMO element of *Pax6* in vivo. (A) Schematic representation of the *Pax6* locus, displaying the exons of *Pax6* (black boxes, top strand) and adjacent *Elp4* gene (black boxes, bottom strand). Ectoderm enhancer (EE) is indicated with red oval; SIMO enhancer is indicated with yellow oval. The detail of the part of the SIMO shows high conservation across the vertebrate species. In SIMO, five putative Meis binding sites were identified with three, SIMO_B, SIMO_C and SIMO_D (indicated with yellow color), clustered in highly conserved part of the SIMO enhancer. (B) The nucleotide composition of selected putative Meis binding sites found in SIMO and their comparison with Meis consensus binding site and previously identified Meis binding site in EE. (C, D) Results of chromatin immunoprecipitation of Meis-bound DNA fragments performed with the mixture of Meis1-specific and Meis2-specific antibody on chromatin prepared from E10.5 whole embryos (C) or α TN4 mouse lens epithelial cells (D) showing clear enrichment on SIMO enhancer. (C, D) Error bars denote SDs, *p and **p versus control using Student's *t*-test.

doi:10.1371/journal.pgen.1006441.g003

DNA constructs containing either the wild-type SIMO enhancer (SIMO WT) or the enhancer simultaneously mutated in conserved Meis binding sites SIMO_B, SIMO_C and SIMO_D (SIMO MUT), respectively, were introduced into the chick eye forming region by *in ovo* electroporation at embryonic stage HH10-11. The electroporated embryos were collected at stage HH20-21 and tested for β -galactosidase activity. As shown in Fig 4C and 4E and S5 Fig, wild-type SIMO enhancer mediated efficient expression of the lacZ reporter gene in the developing chick lens. In contrast, when all three Meis binding sites were mutated in SIMO, the lens-specific activity of the resulting reporter gene construct was abrogated (Fig 4D and 4F and S5 Fig).

Next, we wanted to determine a possible contribution of individual Meis binding sites to SIMO enhancer activity. Mutation of SIMO_B Meis binding site alone resulted in decreased expression of reporter gene in lens as compared to wild-type SIMO, whereas simultaneous mutation of both SIMO_B and SIMO_C binding sites led to a complete loss of lens-specific expression of reporter gene (S6A Fig). These data suggest additive effect of three Meis binding sites on SIMO enhancer activity.

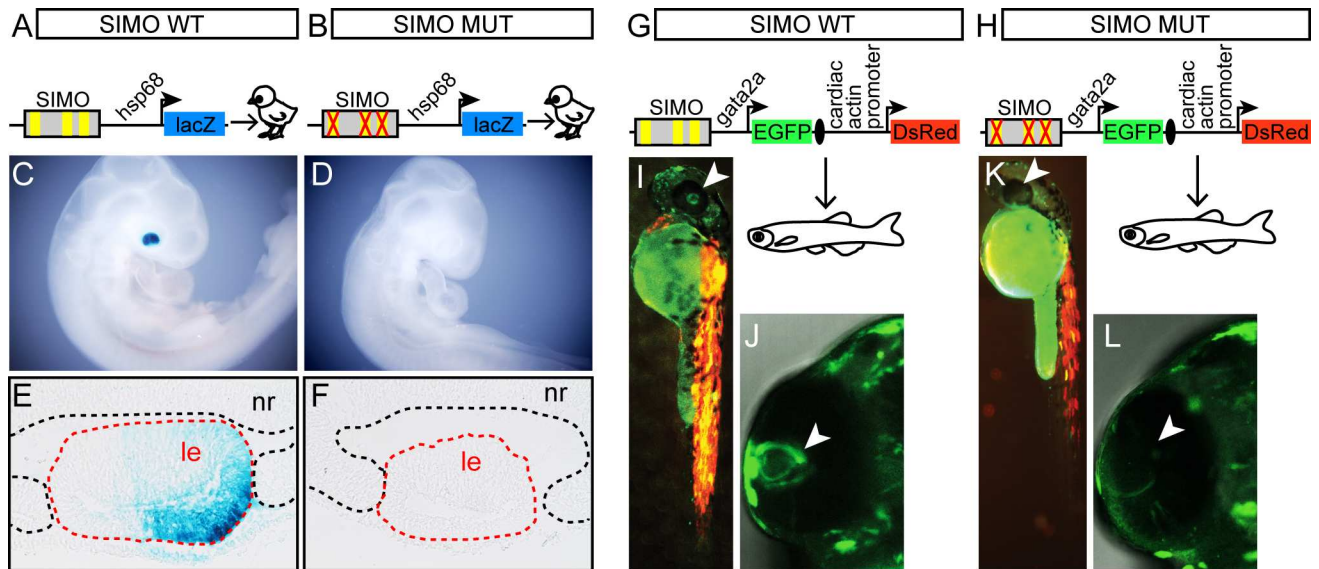


Fig 4. Characterization of SIMO wild-type and mutant enhancer by reporter gene assays in chick and zebrafish. (A, B) Schematic view of reporter constructs used for *in ovo* electroporation of chick embryos. Reporter constructs carry wild-type or mutant mouse SIMO element upstream of *hsp68* minimal promoter and β -galactosidase open reading frame. In mutant SIMO Meis binding sites were abolished by introduction of specific single-point mutations changing Meis recognition sequence TGACAG/A into TcACAG/A. (C–F) Whole-mount view or histological sections through the eye of β -galactosidase-stained chick embryos of stage HH21–22 electroporated either with (C, E) wild-type or with (D, F) mutant SIMO fragment. Positive X-gal staining correlates with the activity of reporter constructs. Wild-type SIMO fragment supports reporter construct expression in lens but not the mutant SIMO fragment. (G, H) Schematic view of reporter constructs used for transgenesis in zebrafish. Reporter constructs carry wild-type or mutant zebrafish SIMO element upstream of zebrafish *gata2a* minimal promoter and EGFP open reading frame. In mutant zebrafish SIMO Meis binding sites were abolished by introduction of specific single-point mutations changing Meis recognition sequence TGACAG/A into TcACAG/A. In order to control for transgenesis efficiency *in vivo* the reporter genes contain a second cassette composed of a cardiac actin promoter driving the expression of a red fluorescent protein (DsRed). EGFP and DsRed transcriptional units are separated by an insulator. (I–L) Wild-type SIMO enhancer activity is detected at 48 hpf (n = 160, 68% EGFP of DsRed positive), (I, J), but not for the mutant construct (n = 36, 89% EGFP negative of DsRed positive) (K, L). LE—lens, NR—neural retina.

doi:10.1371/journal.pgen.1006441.g004

We noticed that Meis binding sites (sequence TGACAA in SIMO_B, SIMO_C and SIMO_D) in wild-type SIMO enhancer do not constitute the perfect match to the optimal Meis DNA-binding site motif TGACAG (<http://jaspar.genereg.net/>) indicating that they might represent a medium affinity sites.

In order to evaluate the functional significance of these non-optimal Meis binding sites for expression in lens we prepared reporter gene constructs expressing *lacZ* gene under the control of a minimal *hsp68* promoter fused to the most conserved region of mouse SIMO enhancer (hereinafter referred to as minSIMO) containing either wild-type or optimized Meis binding sites. As shown in S6B Fig, substitution of wild-type Meis binding sequence in SIMO_B, SIMO_C and SIMO_D for optimal Meis binding sequence motif resulted in higher level of reporter activity in the developing lens. These data are in accord with the key functional role of Meis proteins in SIMO regulation and indicate that strong but restricted SIMO enhancer activity relies on a cluster of three medium affinity non-optimal Meis binding sites. Notably, recent systematic study of a model enhancer shows that enhancer specificity depends on a combination of suboptimal recognition motifs having reduced binding affinities. Conversion of suboptimal binding sites to perfect matches to consensus mediates robust but ectopic patterns of gene expression [39].

Finally, in order to gain further insight into enhancer architecture we used JASPAR database (<http://jaspar.genereg.net/>) to screen throughout the most evolutionarily conserved core region of SIMO (minSIMO region) for consensus binding sites of additional transcription

factors. We identified potential binding sites for Six3, Ets/Tead, Maf and homeodomain-containing transcription factors (S6C Fig). We performed site-directed mutagenesis of SIMO introducing dinucleotide changes in the conserved residues of the consensus binding sites (LOGOs in JASPAR database). In addition, we mutagenized an evolutionarily conserved GCTC box present in SIMO of all species analyzed in Fig 3A. Reporter gene constructs expressing lacZ gene under the control of minimal *hsp68* promoter fused either to the wild-type SIMO enhancer, or to the enhancer mutated in binding site for each particular transcription factor, were introduced into the chick eye forming region by *in ovo* electroporation at embryonic stage HH10-11. As shown in S6C Fig, none of the mutations resulted in a complete abrogation of lens-specific reporter gene activity as did mutations in Meis binding sites SIMO_B and SIMO_C (S6A Fig). Notably, mutation of Six3 binding site resulted in decreased expression of reporter gene (S6C Fig), suggesting the requirement of similar Six3 input in SIMO enhancer as in EE [23]. Mutations in homeodomain binding sites HD1 and HD2 but not in HD3 lead to a subtle decrease of reporter activity (S6C Fig). Taken together, reporter gene assays in chick demonstrated an essential role of Meis transcription factors for SIMO enhancer activity.

Intrigued by the fact that Meis binding sites SIMO_B, SIMO_C and SIMO_D were phylogenetically conserved between mouse and zebrafish we next examined the functional significance of these sites in the context of zebrafish SIMO element. It was previously shown that the region encompassing zebrafish SIMO was able to drive expression to the lens of 48 hpf zebrafish [19]. We made a zebrafish EGFP reporter gene transgenic using wild-type and Meis-mutated versions of zebrafish SIMO element fused to minimal *gata2a* promoter (Fig 4G and 4H). In order to control for successful transgenesis and to quantitate results between the two constructs, ZED vector containing surrogate muscle-specific DsRed marker gene separated from EGFP reporter gene by an insulator was used [40]. In accordance with a previous study [19], transgenic fish carrying wild-type SIMO enhancer exhibited high level of EGFP in the lens at 48hpf (Fig 4I and 4J). In contrast, mutation of the phylogenetically conserved Meis binding sites resulted in the loss of EGFP due to the loss of lens-specific enhancer activity of SIMO while the muscle-specific surrogate reporter gene was still active (Fig 4K and 4L). These results suggest an evolutionarily conserved role of Meis proteins in the regulation of the *Pax6* SIMO enhancer. Combined, our data establish that the SIMO enhancer is a natural target of Meis1 and Meis2 and that this physical interaction conveys expression of *Pax6* in developing vertebrate lens.

Genetic ablation of SIMO and EE *in vivo*: an insight into *Pax6* enhancer redundancy

In order to get an insight into SIMO function *in vivo* we generated mice carrying deletion of its evolutionarily conserved central core. Targeted engineering of genomic DNA in *Pax6* locus was achieved using a pair of transcription activator-like effector nucleases (TALENs) designed to delete approximately 200 bp of the most evolutionarily conserved core region of SIMO (S7A Fig). Several lines of mice were established (S7B Fig) from which the line #710 designated $Pax6^{SIMOdel710/+}$ was used for most of further studies. Enhancer region deleted in line #710 encompass *Pax6* autoregulatory element and Meis1/2 binding sites SIMO_B, SIMO_C and SIMO_D, respectively, and is absolutely required for lens-specific activity based on transgenic reporter assay in chick (S7C Fig). To our surprise, mice carrying a homozygous deletion of SIMO ($Pax6^{SIMOdel710/SIMOdel710}$) did not manifest a major lens developmental phenotype (S7D Fig). To test whether lowering the dose of *Pax6* may phenotypically uncover SIMO function during early lens development, we combined $Pax6^{SIMOdel710/+}$ allele with *Sey* allele (*Pax6*

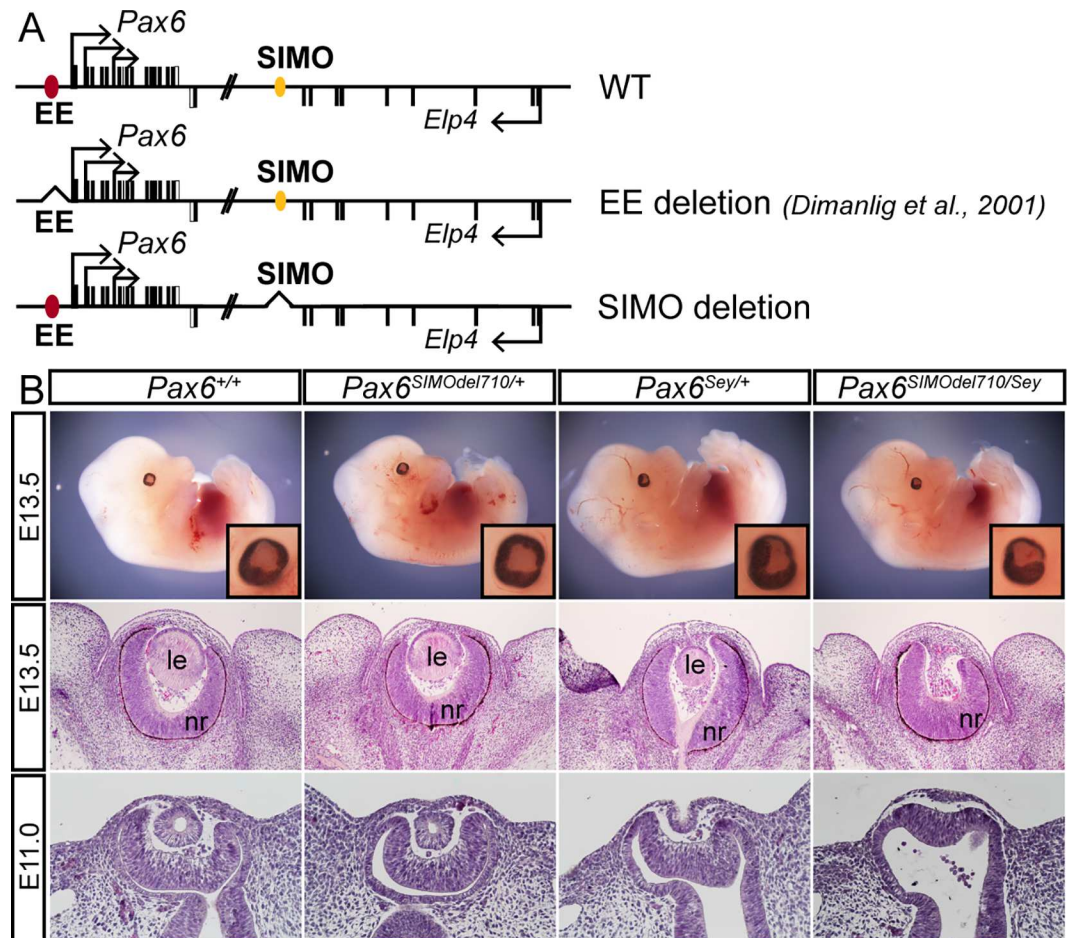


Fig 5. Genetic analysis of SIMO deletion *in vivo*. (A) Scheme of wild-type *Pax6* locus and alleles carrying EE [17] or SIMO deletion (this study). EE is indicated with red oval and SIMO with yellow oval. (B) Phenotypic consequences of SIMO deletion in *Pax6*^{SIMOdel710/Sey} compound heterozygote mice. Whole-mount view of E13.5 embryos of the indicated genotype with eye in the inset (top panel). Histological sections through the eye demonstrating the absence of lens at E13.5 (middle panel) and arrested development prior to lens pit stage at E11.0 in *Pax6*^{SIMOdel710/Sey} embryos. nr—neural retina, le—lens.

doi:10.1371/journal.pgen.1006441.g005

loss-of-function), (Fig 5). Under these conditions, only one allele of *Pax6* carries SIMO enhancer deletion, while the second is genetically inactive in *Sey*. Although there are several lens phenotypes associated with the complete inactivation of one *Pax6* allele in *Sey* mice, lens is always formed [5, 6], (Fig 5B). Remarkably, when the function of the second allele of *Pax6* in *Sey* mice is compromised by SIMO deletion, lens development is arrested prior to lens pit stage (Fig 5B, the bottom panel) and no lens is detected in compound *Pax6* heterozygote embryos at E13.5 (Fig 5B, the middle panel).

Finally, to demonstrate redundant role of *Pax6* enhancers EE and SIMO for lens induction, we generated mice carrying deletion of both enhancers SIMO and EE simultaneously. For that purpose, we used CRISPR/Cas9 system to delete approximately 500 bp long critical region of EE [15, 16] on the *Pax6*^{SIMOdel710/SIMOdel710} genetic background. Several transgenic lines of *Pax6*^{ΔEE;ΔSIMO/ΔEE;ΔSIMO} mice were established (hereinafter referred to as *Pax6*^{EE/SIMO} double mutant), from which line containing 477bp deletion of EE simultaneously with SIMO deletion was used for further analysis (Fig 6A). Histological analysis of mice lacking all four copies of lens enhancers at E11.0 revealed arrest of lens development prior to lens pit formation

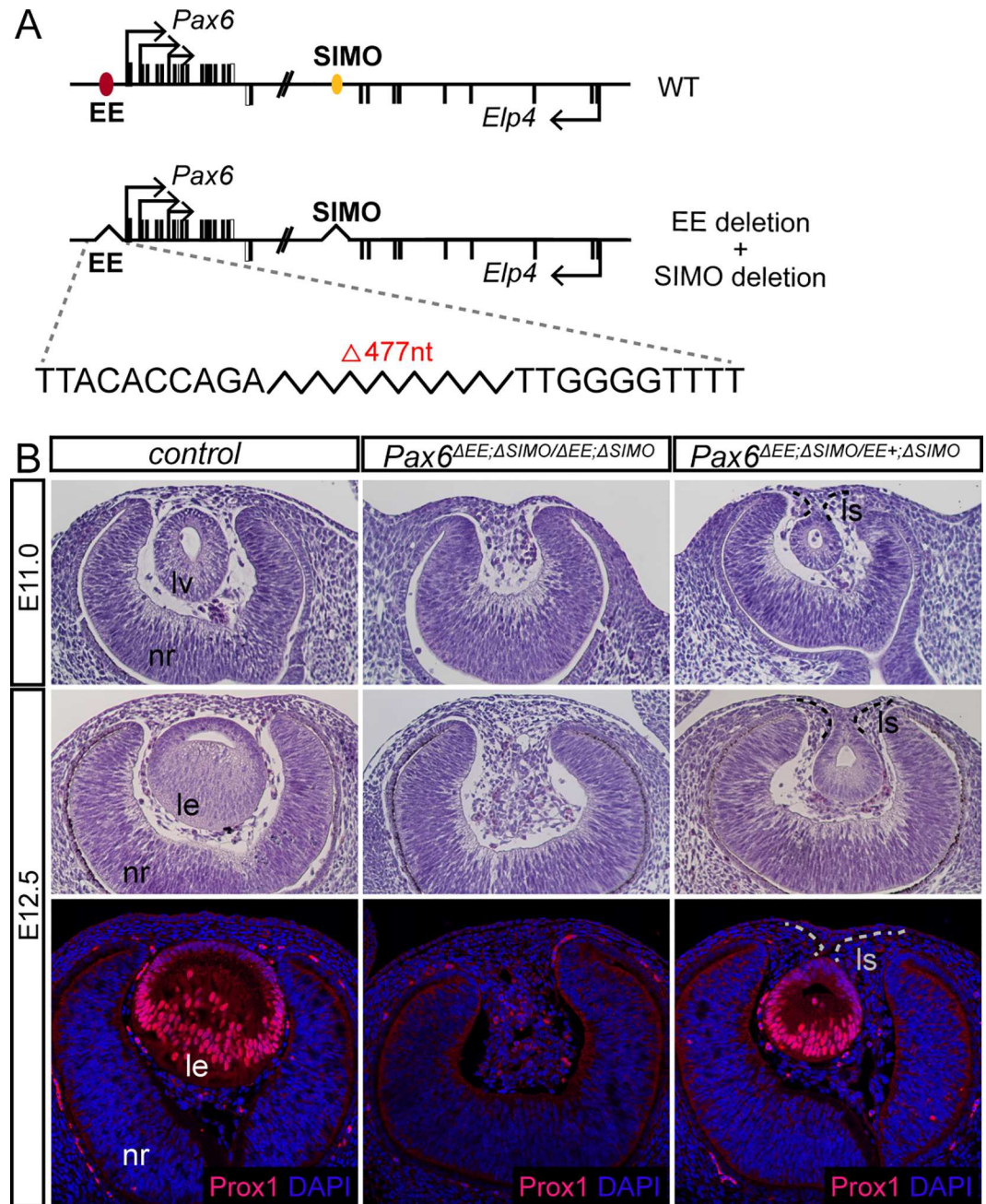


Fig 6. Genetic analysis of the simultaneous deletion of EE and SIMO *in vivo*. (A) Scheme of wild type *Pax6* locus, and allele carrying simultaneous deletion of EE and SIMO. EE is indicated with red oval and SIMO with yellow oval. The exact borders of EE deletion are specified by nucleotide sequences flanking the deletion. (B) Phenotypic consequences of simultaneous deletion of EE and SIMO in *Pax6*^{ΔEE;ΔSIMO/ΔEE;ΔSIMO} embryos. Hematoxylin and eosin stained paraffin sections demonstrating the arrested lens development prior to lens pit stage at E11.0 and absence of lens at E12.5 in *Pax6*^{ΔEE;ΔSIMO/ΔEE;ΔSIMO} embryos. Immunofluorescent staining for lens marker Prox1 is not detected in E12.5 *Pax6*^{ΔEE;ΔSIMO/ΔEE;ΔSIMO} embryos. Note that a single allele of intact EE in *Pax6*^{ΔEE;ΔSIMO/EE+;ΔSIMO} embryos is sufficient for lens formation albeit the resulting lens is much smaller compared to control, and lens stalk is apparent. nr—neural retina, lv—lens vesicle, le—lens, ls—lens stalk.

doi:10.1371/journal.pgen.1006441.g006

(Fig 6B). Immunofluorescent staining for lens marker Prox1 at E12.5 confirmed the absence of lens tissue in *Pax6*^{EE/SIMO} double mutant embryos (Fig 6B, the bottom panel). Remarkably, a

single copy of a functional enhancer in *Pax6*^{ΔEE;ΔSIMO/EE+;ΔSIMO} embryo was sufficient for lens induction albeit the resulting lens was much smaller at E11.0 as compared to control and lens stalk was apparent in *Pax6*^{ΔEE;ΔSIMO/EE+;ΔSIMO} mice at E12.5 indicating delayed development (Fig 6B).

Genetic data indicated redundancy as well as potential additive activity of EE and SIMO. To provide further evidence that both EE and SIMO might be additively required for high level of *Pax6* expression during lens induction we tested synergistic role of SIMO and EE on strength and specificity of expression of reporter genes in the developing chick lens. For that purpose we used reporter gene constructs expressing lacZ gene under the control of a minimal *hsp68* promoter fused to either SIMO alone, EE alone, or combination of both enhancers (S8 Fig). As expected, combination of full-length EE [16] with SIMO elicited stronger expression of lacZ reporter gene than did SIMO alone (S8B Fig). Similarly, combination of minimal functional EE [15] with the most conserved region of SIMO (minSIMO) ensured stronger expression than did either of the minimal enhancers alone (S8C Fig). Strong and specific reporter gene activity may also be achieved by duplication of the same type of enhancer (S8C Fig). Reporter gene assays suggest that simultaneous use of both EE and SIMO enhancers may be beneficial for achieving high-level tissue-specific *Pax6* gene expression during lens induction.

Combined, our data demonstrate simultaneous requirement of EE and SIMO *Pax6* enhancers for normal lens development and provide evidence of their apparent redundancy and synergistic activity at early stages of lens induction.

Discussion

GRNs provide a system level explanation of development in terms of the genomic regulatory code [41, 42]. While significant insights into the functional role of many transcription factors during the lens placode formation have been realised, much less is known about the upstream regulation of these critical factors and the intricate wiring of the GRN that controls the earliest stages of lens development. Previous studies have shown that the GRN of mammalian lens induction is governed by a multitude of mutual cross-regulations, including the transcription factors *Pax6*, *Six3* and *Sox2* (summarized in the BioTapestry visualization Fig 7). *Six3* appears to regulate the onset of *Pax6* expression in the PLE while *Pax6* subsequently maintains *Six3* levels [23, 35, 43]. Only a small fraction of *Six3*^{fl^{del}}; *Le-Cre* embryos, type III in [23], exhibit a complete arrest of lens development prior to the lens pit stage, a phenotype comparable to *Pax6* knockout phenotype, although this might be due to the inefficient deletion of *Six3*. Consequently, the level of *Six3* ablation in lens-derived tissue correlates well with the grade of phenotype and *Pax6* and *Sox2* downregulation [23]. Epistasis of *Pax6* and *Sox2* is stage-dependent. In pre-placodal ectoderm, *Pax6* and *Sox2* are regulated independently. By contrast, after the lens placode has formed, *Sox2* expression is dependent on *Pax6* [34]. Genetic data presented here reveal a fundamental and redundant role of *Meis1* and *Meis2* homeoproteins in the regulation of lens induction. *Meis1* and *Meis2* transcription factors have previously been identified as upstream regulators of the *Pax6* EE [22]. However, *Meis1*- and EE-deficient mice surprisingly do not display eye phenotypes at placodal stage of lens development [17, 28] and therefore are not comparable to that of the lens-specific ablation of *Pax6* [7]. This indicates that (i) *Meis2* may compensate for the loss of *Meis1*, and that (ii) another *Pax6* enhancer driving expression to lens may substitute for missing EE [17, 44]. Until recently, interrogation of the combined role of *Meis1/2* proteins on lens induction and *Pax6* expression *in vivo* has been hampered by the lack of suitable *Meis2* knockout allele. Herein, we have conducted a comprehensive genetic analysis of *Meis1* and *Meis2* function in mouse to show that simultaneous depletion of *Meis1* and *Meis2* in the presumptive lens ectoderm results in the failure of lens

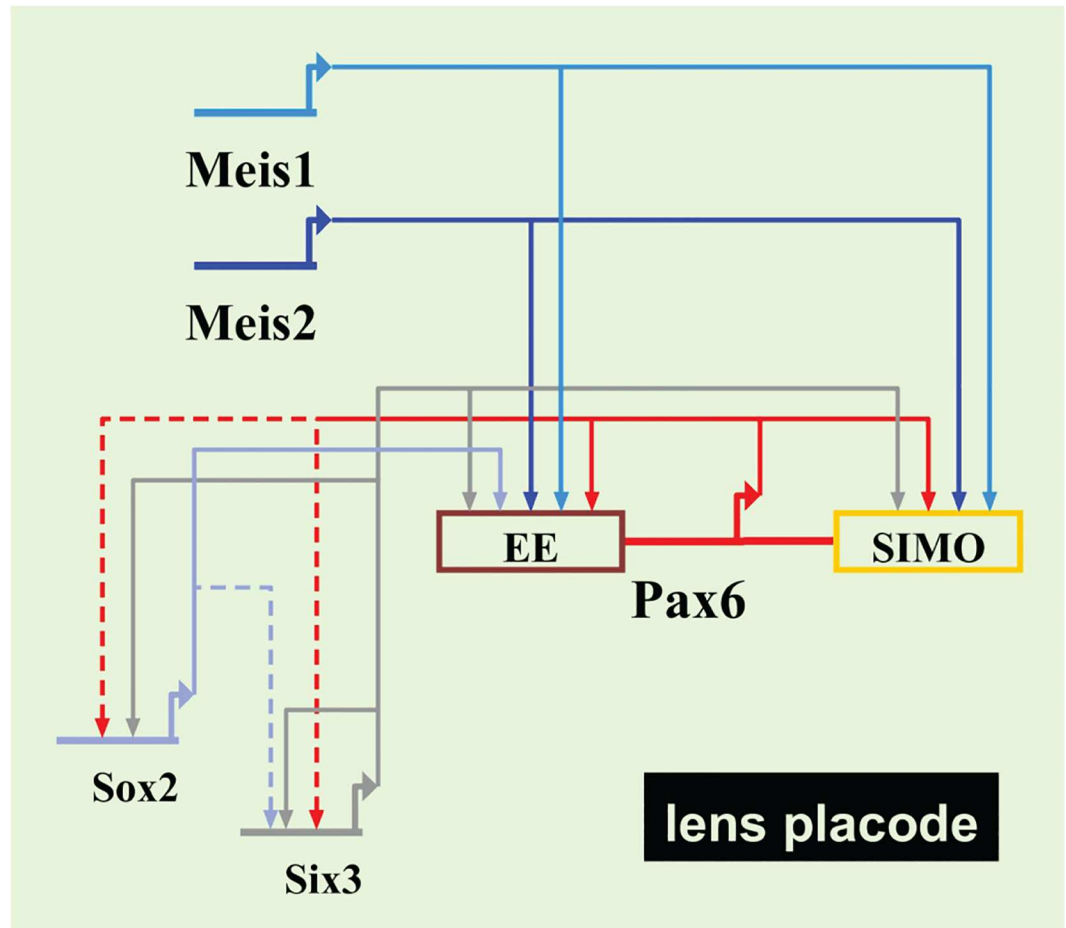


Fig 7. Current model of transcriptional regulatory network operating during mammalian lens induction. Direct interactions are indicated with solid lines, whereas dashed lines show possible direct interactions inferred from gain- and loss-of-function studies.

doi:10.1371/journal.pgen.1006441.g007

placode formation and a marked reduction of *Pax6* and *Six3* expression in the presumptive lens areas. In contrast, expression of *Sox2* is maintained in the *Meis1/Meis2* mutated ectoderm. The Meis-related TALE homeodomain protein *Prep1* (also known as *Pknox1*) appears to control the timing of *Pax6* activation and its expression level in the developing lens via direct binding to the EE [25]. The available data regarding the genetic requirement for *Prep1* suggest it has a cell-nonautonomous function in lens induction. *Prep1* trans-heterozygotes composed of a germline knockout and retroviral insertion allele (a hypomorph), respectively, demonstrate defects at the lens induction step [25]. In contrast, conditional gene targeting of *Prep1* at pre-placodal and placodal phases of lens induction using *Ap2alpha-Cre* and *Le-Cre* did not reveal any developmental phenotype [45]. We were unable to detect any changes in *Prep* expression using immunohistochemistry (S9 Fig), making it unlikely that the observed phenotype in *Meis1/2* double knockout mice is due to *Prep1* deficiency.

Our data are consistent with the scenario in which *Meis1/2* function as regulators of lens placode development primarily via activation of *Pax6* enhancers. However, it is likely that *Meis1* and *Meis2* regulate other factors contributing to early lens development such as the ones identified for *Meis1* [46]. It was recently shown that *Meis1* regulates either directly or

indirectly the expression of genes involved in patterning, proliferation and differentiation of the neural retina, and that haploinsufficiency of *Meis1* causes microphthalmic traits and visual impairment in adult mice [46]. Based on the fact that Marcos et al. could not detect *Meis2* expression at early stages of eye development, authors considered only *Meis1* function to be critical for early mouse eye development [46]. In contrast, in this study we detected *Meis2* expression in early stages of lens development (S1 Fig). Furthermore, *Meis2* expression is lost upon genetic ablation of *Meis2* gene (S1J Fig). This data together with the fact that only simultaneous deletion of *Meis1* and *Meis2* in PLE leads to an arrest of lens development in pre-placodal stage strongly suggests that both *Meis1* and *Meis2* are expressed and essential for early eye development. Nevertheless, it is very likely that *Meis1* and *Meis2* fulfill the redundant function only in specific developmental stages and processes (our data and [46]), while having many discrete functions in the embryo even within the eye development.

Mammalian eye development is highly sensitive to the levels of *Pax6* as haploinsufficiency causes aniridia in humans and multiple ocular defects in mice [4, 47–50]. In contrast, increased levels of *Pax6* result in various ocular abnormalities [51]. In the mammalian lens, *Pax6* controls all known steps of tissue morphogenesis [7, 34, 52] but its dosage appears to be especially critical during the earliest developmental stages. The data presented here show that the molecular mechanisms of *Meis1/2* regulation of *Pax6* are mediated by at least two "shadow enhancers" (Fig 7): a 3'-located ultraconserved SIMO identified as a *Meis* target here, and a 5'-located ectoderm enhancer (EE), identified as a target of TALE proteins earlier [22, 25]. The concept of the seemingly redundant "shadow enhancers" driving expression of a given gene to overlapping or identical patterns has been pioneered in *Drosophila* as a potential source of evolutionary novelty [53]. It was hypothesized that "shadow enhancers" may evolve novel binding sites and achieve new regulatory activities without disrupting the core patterning function of a developmental control gene. As cis-regulatory mutations are the main driving force of animal evolution [54, 55] buffering loss-of-function situations during enhancer evolution may be critical. "Shadow enhancers" analyzed in detail in *Drosophila* to date provide robustness and precision to the system [56–58]. A remote "shadow enhancer" identified in the human *ATOH7* gene, by virtue of its deletion in patients suffering with nonsyndromic congenital retinal non-attachment, displays identical spatiotemporal activity to the primary enhancer when tested by transgenesis [59]. Although the function of the primary and "shadow enhancer" are not firmly established, dual enhancers may reinforce *Atoh7* expression during early critical stages of eye development when retinal neurogenesis is initiated. It is tempting to speculate that the two apparently redundant distal "shadow enhancers" (EE, SIMO) ensure robust and tight regulation of *Pax6* gene expression during mammalian lens induction. In our view robustness of *Pax6* "shadow enhancer" system provides stable high level of *Pax6* gene expression and confers compensation for deleterious effects and protection to expression level fluctuations due to environmental influences. Recent systematic analysis of "shadow enhancers" during *Drosophila* mesoderm development revealed that their spatio-temporal redundancy is often partial in nature, while the non-overlapping function may explain why these enhancers are maintained within a population [60]. Reporter gene assays and genetic ablation experiments shown here provide evidence for redundant ("shadow") enhancer function of SIMO and EE selectively during early stages of lens induction. Later on the two enhancers may indeed act more independently with some overlap of transcription factor use while their distinctness is likely elicited by different sets of transcription factors co-expressed and co-bound at different times and in different combinations and stoichiometry. It is nevertheless intriguing that the two enhancers responsible for lens placode expression of *Pax6* utilize similar molecular logic, namely *Meis1/2*-dependency ([22] and this study), *Six3* regulatory input ([23] and this study) and autoregulatory function [19, 21]. Furthermore, two *Meis/Prep* binding sites, L1 and L2, were identified in

the EE [22, 25] while at least three evolutionarily conserved Meis binding sites are present in SIMO (this study). In theory, the accumulation of homotypic binding sites may aid the enhancer robustness and may protect the enhancer from vulnerable mutations leading to the loss of responsiveness to a particular transcriptional regulator. Phylogenetic footprinting and reporter gene transgenics indicate that SIMO enhancer activity in zebrafish not only depends upon *Pax6* autoregulation [19] but also on functional Meis binding sites (this study). Given the profound difference in the early stages of lens development in mice (lens formed by invagination) and fish (lens arises by delamination) it is remarkable that the SIMO enhancer maintains its Meis-dependent regulation albeit not for the comparable developmental stage. In fact, SIMO enhancer becomes active in zebrafish only at 48 hours post fertilization when the lens is already formed [19]. This illustrates that species-specific adaptation of enhancer function is combined with a developmental change. It will be interesting to see if other features of SIMO regulation, such as Six3 interaction, are maintained in zebrafish. No functional data exist for the zebrafish EE, although at the sequence level this regulatory element is evolutionarily conserved from human to fish [13, 15, 25]. It remains to be seen if the evolutionary strategy of maintaining lens "shadow enhancers" in the *Pax6* locus is utilized in zebrafish, or the developmental robustness is achieved via *Pax6* gene duplication giving rise to *Pax6.1a* and *Pax6.1b* paralogues [61].

Pax6 is considered as an extreme case of an evolutionarily conserved developmental regulator promoting eye formation in vertebrates and *Drosophila* [62]. Meis genes belong to the TALE homeobox family found in genomes across all Metazoa [63]. In contrast to *Pax6*, *Homothorax*, a *Drosophila* orthologue of vertebrate *Meis/Prep* genes, suppresses eye development rather than promoting it [64]. *Homothorax* together with the Cut homeoprotein suppresses expression of *Pax6* orthologue *Eyeless* in the antenna disc [65]. Conversely, *Sine oculis*, a downstream target of *Eyeless*, suppresses *Homothorax* and *Cut* in the eye disc thus allowing eye development to proceed [65]. The different genetic wiring of *Pax6/Eyless* and *Meis/Homothorax* in vertebrate and *Drosophila* eye developmental programs may merely reflect the vast evolutionary distance between the respective species, morphological differences in the eye types being built and a general strategy of re-purposing individual components from the common genetic toolkit during the course of evolution.

In conclusion, this study identifies a genetic requirement for *Meis1* and *Meis2* for early steps of mammalian eye development and reveals an apparent robustness of the gene regulatory mechanism whereby two independent "shadow enhancers" of similar molecular architecture maintain critical levels of a dosage-sensitive gene, *Pax6*, during lens induction. These results allow us to establish a genetic hierarchy during early vertebrate eye development and provide novel mechanistic insights into the regulatory logic of this process.

Materials and Methods

Ethics statement

Housing of mice and *in vivo* experiments were performed in compliance with the European Communities Council Directive of 24 November 1986 (86/609/EEC) and national and institutional guidelines. Animal care and experimental procedures were approved by the Animal Care Committee of the Institute of Molecular Genetics (study #174/2010). Mice were sacrificed by cervical dislocation.

Mice

To inactivate *Meis1*, *Meis1*^{+/-} [28] mice were used. A conditional mutant allele of the *Meis2* gene (*Meis2*^{ff}) was generated by inserting loxP sites in the introns 2 and 6, flanking exons 3

and 6 in the *Meis2* gene (S1G Fig) at the Gene Targeting & Transgenic Facility, University of Connecticut, USA [32]. To generate whole-body knockout of *Meis2*, *Meis2*^{fl/fl} mice were crossed with *Hprt-Cre* mice (strain 129S1/Sv-Hprt^{tm1(Cre)Mnn}/J, stock 004302, The Jackson Laboratory) that display the zygotic *Cre* recombinase activity. For specific deletion of *Meis2* in presumptive lens ectoderm, *Le-Cre* [7] mice were used. ROSA26R [66] and *Pax6*^{Sey-1^{Neu}} [4] mice (herein designated as *Pax6*^{Sey/+}) have been described previously. SIMO enhancer was deleted using a pair of TALENs targeting sequences TCAGCCCCACCCATACTCtcaaaggaatgtcgTCGAGCGT CAGTGCCTGAA and TGCACCTGTCACTCAGCATTAtccatcctcattaaTGACAATGGGAA AGTTTA (recognition sequence shown in capital letters). TALENs were designed using TAL Effector Nucleotide Targeter 2.0 (<https://tale-nt.cac.cornell.edu/>), assembled using the Golden Gate Cloning system [67], and cloned into the ELD-KKR backbone plasmid [68]. Polyadenylated TALEN mRNAs were prepared using mMESSAGE mMACHINE T7 ULTRA Kit (Ambion) and were injected into the cytoplasm of fertilized mouse oocytes. EE [16] was deleted using CRISPR/Cas9 system. A sequence containing EE region was submitted to CRISPR Design Tool (<http://crispr.mit.edu/>) to select for a set of sgRNAs. Oligonucleotides used to make sgRNA constructs are listed in S1 Table and were cloned into pT7-gRNA (pT7-gRNA was a gift from Wenbiao Chen, Addgene plasmid # 46759). Cas9 mRNA was prepared using mMESSAGE mMACHINE T7 ULTRA Kit (Ambion) using plasmid pCS2-nCas9n (pCS2-nCas9n was a gift from Wenbiao Chen, Addgene plasmid # 47929). The sgRNAs were transcribed using MEGAscript kit (Ambion). A mixture of Cas9 mRNA (100ng/μl) and specific sgRNAs (25ng/μl each) was injected into the cytoplasm of fertilized mouse oocytes with homozygous or heterozygous deletion of SIMO enhancer (genetic background *Pax6*^{SIMOdel710/SIMOdel710} or *Pax6*^{SIMOdel710/+}). Multiple independent lines were established and the extent of EE deletion was analysed in F1 animals by DNA sequencing.

Tissue collection, histology and immunohistochemistry

Mouse embryos were staged by designation the noon of the day when the vaginal plug was observed as embryonic day 0.5 (E0.5). Embryos of desired age were dissected, fixed in 4% paraformaldehyde (PFA) from 45 minutes up to 4 hours at 4°C, washed with PBS, cryopreserved in 30% sucrose and frozen in OCT (Sakura). The cryosections (10–12 μm) were permeabilized with PBT (PBS with 0.1% Tween), blocked with 10% BSA in PBT and incubated with primary antibody (1% BSA in PBT) overnight at 4°C. Sections were washed with PBS, incubated with fluorescent secondary antibody (Life Technologies, 1:500) for one hour at room temperature, washed with PBS, counterstained with DAPI and mounted in Mowiol. The images were taken on Leica SP5 confocal microscope and were processed (contrast and brightness) with Adobe Photoshop. For hematoxylin-eosin staining, embryos were fixed in 8% PFA overnight, processed, embedded in paraffin, sectioned (8 μm), deparaffinized and stained. For β-galactosidase staining, embryos were fixed in 2% PFA, washed with rinse buffer (0.1 M phosphate buffer pH 7.3, 2 mM MgCl₂, 20 mM Tris pH 7.3, 0.01% sodium deoxycholate, and 0.02% Nonidet P-40) and incubated in X-Gal staining solution (rinse buffer supplemented with 5 mM potassium ferricyanide, 5 mM potassium ferrocyanide, 20 mM Tris pH 7.3, and 1 mg/ml X-gal) at 37°C for 2 hours and at room temperature overnight shaking.

Chromatin immunoprecipitation

For chromatin immunoprecipitation whole E10.5 embryos or murine lens epithelial cells αTN4 [37] were used. A chromatin immunoprecipitation assay was performed according to manufacturer's protocol (Upstate Biotech) with slight modifications as previously described

[69]. The assay was repeated twice for both embryonic and tissue culture samples. The immunoprecipitated DNA was analyzed by qRT-PCR.

Electrophoretic mobility shift assay

In silico analysis to identify putative Meis binding sites in *SIMO* was performed using high-quality transcription factor binding profile database JASPAR [70]. Electrophoretic mobility shift assays (EMSAs) was performed using double-stranded oligonucleotides comprising binding sites *SIMO_B*. A single point mutation was introduced into binding site changing Meis recognition sequence TGACAG/A into TcACAG/A. ³²P-labeled oligonucleotides were incubated with *in vitro*-synthesized FLAG-Meis2 (TNT Quick, Promega) in binding buffer (10 mM HEPES pH 7.9, 100 mM KCl, 1mM EDTA, 4% Ficoll, 0.05mg/mL poly-dIdC) at room temperature for 15 minutes. For supershift experiment, anti-FLAG M2 antibody was included in the binding reaction. Samples were analysed by 6% polyacrylamide gel electrophoresis and autoradiography.

Electroporation *in ovo*

The wild-type mouse *SIMO* enhancer was amplified from genomic DNA using primers shown in [S1 Table](#) and introduced into the electroporation vector containing hsp68-lacZ reporter cassette [20]. Transcription factor binding sites within *SIMO* were mutagenized using QuickChange mutagenesis kit (Stratagene). Constructs carrying minimal EE and minimal *SIMO* enhancers were generated using synthetic double stranded oligonucleotides shown in [S1 Table](#). All reporter gene constructs were verified by DNA sequencing. Brown Leghorn eggs were incubated until reaching HH10–11 stages and electroporation was performed as described [71]. The DNA mixture was injected outside of the right developing optic cup and electroporated using voltage of 12 V, length of pulse 20 ms, interval length 100 ms. The embryos were collected in stage HH20–HH21, fixed for 15 minutes in 2% formaldehyde and proceeded to X-gal staining.

Zebrafish transgenesis

The wild-type zebrafish *SIMO* enhancer was introduced into ZED vector upstream of minimal *gata2a* promoter [40]. Meis binding sites within *SIMO* were mutagenized using QuickChange mutagenesis kit (Stratagene). For transgenesis, the Tol2 transposon/transposase method [72] was used with minor modifications. A mixture containing 30 ng/μl of transposase mRNA, 30 ng/μl of Qiagen column purified DNA, and 0.05% phenol red was injected in the cell of one-cell stage embryos. Embryos were raised at 28.5 °C and staged by hours post fertilization (hpf). Embryos selected for imaging were anaesthetised with tricaine and mounted in low-melting agarose. Images were taken on Leica SP5 confocal microscope.

Oligonucleotides and antibodies

All used oligonucleotides are listed in [S1 Table](#). All used primary antibodies are listed in [S2 Table](#).

Supporting Information

S1 Fig. Meis1 and Meis2 are co-expressed throughout early lens development. *Le-Cre*-mediated Meis2 elimination from presumptive lens ectoderm. (A–F) Cryosections from wild-type embryos of the indicated ages labeled for Meis1 and Meis2. (A, B) At E9.5, both Meis1 and Meis2 are expressed in lens placode (LP), and surrounding head surface ectoderm

(SE) of wild-type embryo. *Meis1* is also detected in optic vesicle (OV) and *Meis2* in mesenchymal cells (MC). (C) At E10.5, *Meis1* is present in lens pit (Lpi), surrounding SE, neural retina (NR) and retinal pigmented epithelium (RPE). (D) *Meis2* expression is present in lens pit, retinal pigmented epithelium and weakly in neural retina. (E) At E11.5 *Meis1* expression persists in SE, lens vesicle (LV), RPE and in some cells of NR. (F) *Meis2* is detected in SE, LV, RPE and peripheral NR. (G) Schematic representation of targeted *Meis2* locus with marked positions of inserted loxP sites. (H, I) *Le-Cre* activity is demonstrated using the *ROSA26R* reporter mouse line. Whole-mounts or sections were stained with X-gal at E9.5 to show *Cre* activity in the eye primordium. (J) Left: Immunofluorescence signal showing *Meis2* expression in surface ectoderm (SE) and lens placode (LP) in section of E9.5 control embryo. Right: Region with inactivated *Meis2* is indicated with a dashed line in section of E9.5 *Meis2* mutant.

(TIF)

S2 Fig. *Meis2* whole-body knockout embryos do not exhibit lens phenotype at E12.5. (A, B) External eye of E12.5 *Meis2*^{-/-} embryo appears comparable to control eye (magnification of eye in insets). (C, D) Hematoxylin-eosin-stained sections at E12.5 do not demonstrate any obvious changes of lens size or morphology in *Meis2*^{-/-} embryos. le – lens.

(TIF)

S3 Fig. Lens specific proteins are not present in E12.5 *Meis1/Meis2* double mutant embryos. (A-L) Cryosections from E12.5 control and *Le-Cre;Meis1*^{-/-};*Meis2*^{fl/fl} embryos stained with antibody as indicated, and nuclei counterstained with DAPI. (B) In *Meis1/Meis2* double mutants expression of *Pax6* is maintained only in neural retina and retinal pigmented epithelium (RPE), since lens is not formed. (D, F, H, J) Note, that lens specific proteins (α - and γ -crystallin, *Prox1*, *Foxe3*) are not detected in sections of *Le-Cre;Meis1*^{-/-};*Meis2*^{fl/fl} embryos. (L) Two separate populations of cells expressing either neural retina (*Sox2*) or RPE (*Otx2*) specific markers are detected in *Meis1/Meis2* double mutant. Scale bars indicate 100 μ m. le-lens, nr-neural retina, rpe-retinal pigmented epithelium.

(TIF)

S4 Fig. *Meis2* binds SIMO enhancer *in vitro* using electrophoretic mobility shift assays (EMSA). FLAG-tagged *Meis2* binds wild-type SIMO_B and can be supershifted by an anti-FLAG antibody. No interaction is detected when a single point mutation is introduced into SIMO_B binding site changing *Meis* recognition sequence TGACAA into TcACAA.

(TIF)

S5 Fig. Overview of SIMO wild-type and mutant enhancer activity in chick. (A) Overview of whole-mount X-gal staining of chick embryos electroporated with reporter construct containing either wild-type or mutant SIMO fragment. (B) Histological sections through the eye of depicted chick embryos. (C) Quantification of positive and negative X-gal (*lacZ*) staining in electroporated chick embryos.

(TIF)

S6 Fig. Characterization of SIMO enhancer mutants by reporter gene assays in chick. (A-C) Wholemout X-gal stained chick embryos (at HH20-21) showing the expression of *lacZ* reporter gene under the control of minimal *hsp68* promoter fused to wild-type or mutated mouse SIMO electroporated into chick eye forming region at developmental stage HH10-11. The numbers of embryos displaying expression pattern shown are indicated in each panel. (A) Contribution of individual *Meis* binding sites to SIMO enhancer activity. Reporter gene constructs carrying wild-type SIMO (SIMO WT), SIMO mutated in a single *Meis* binding site (SIMO MUT-SIMO_B), or two *Meis* binding sites (SIMO MUT-SIMO_BC) were used for

electroporation *in ovo*. Whole-mount X-gal staining demonstrate the effect of mutated Meis binding sites on expression of reporter gene. Cryosections through eye region illustrate a marked decrease of lacZ expression when a single Meis binding site (SIMO_B) was mutated, and a complete loss of lens-specific expression when two Meis binding sites (SIMO_BC) were mutated. **(B)** Optimized Meis binding sites increase the activity of SIMO enhancer. Reporter gene constructs carrying either minimal wild-type SIMO (minSIMO WT), or minimal SIMO in which natural Meis binding sites TGACAA were substituted with optimized binding sequence TGACAG (minSIMO optimalMeis) were used for electroporation *in ovo*. Whole-mount X-gal staining shows that the presence of optimized Meis binding sites in SIMO moderately increases the expression of reporter gene. **(C)** The effect of selected mutations in potential transcription factor binding sites on SIMO enhancer activity. DNA constructs containing either the wild-type SIMO (SIMO WT), or the enhancer carrying mutations in binding sites for the indicated transcription factor were used for electroporation *in ovo*. Schematic pictures of transcription factor binding motifs are taken from JASPAR database. Mutated nucleotides in binding site of each transcription factor are highlighted in small red letters. nr – neural retina, le – lens.

(TIF)

S7 Fig. Generation and characterization of mice carrying SIMO deletion. **(A)** Schematic representation of the *Pax6* locus, displaying the exons of *Pax6* (black boxes, top strand) and adjacent *Elp4* gene (black boxes, bottom strand). Ectodermal enhancer (EE) is indicated with red oval; SIMO enhancer is indicated with yellow oval. The relative position of TALEN recognition sequences is shown with regards to *Pax6* autoregulatory element [19], shaded grey and Meis1/2 binding sites SIMO_B, SIMO_C and SIMO_D (all shaded yellow). **(B)** Schematic representation and PCR genotyping of deletions in individual lines of mice characterized (line number is indicated in red box). **(C)** Whole-mount view of β -galactosidase-stained chick embryos of stage HH21-22 electroporated either with wild-type or with mutant SIMO carrying a deletion found in line #710. Positive X-gal staining correlates with the activity of reporter constructs. **(D)** Histological sections of E11.5 and E13.5 control and *Pax6*^{SIMOdel710/SIMOdel710} embryonic eyes.

(TIF)

S8 Fig. Additive lens specific enhancer activity is observed for EE and SIMO. **(A)** Schematic representation of the *Pax6* locus, displaying the exons of *Pax6* (black boxes, top strand) and adjacent *Elp4* gene (black boxes, bottom strand). Ectodermal enhancer (EE) is indicated with red oval; SIMO enhancer is indicated with yellow oval. **(B,C)** Reporter gene constructs (depicted with schematic view) carrying either SIMO alone, EE alone, or enhancer combinations were used for electroporation to reveal impact of these *Pax6* enhancers for strength and specificity of expression. Combinations of EE and SIMO (EE + SIMO, minEE + minSIMO) ensure stronger expression of reporter gene as compared to SIMO alone or EE alone. While minimal EE (minEE) drives stronger expression of reporter gene than minimal SIMO (minSIMO), the two copies of minSIMO enhancer (minSIMO 2x) provides the strongest reporter gene expression of enhancer variants tested in this experiment. The numbers of embryos displaying expression pattern shown are indicated.

(TIF)

S9 Fig. Prep expression is not changed in *Meis1/Meis2* double mutant embryos. **(A, B)** Cryosections through eye region of E10.5 control and *Le-Cre;Meis1*^{-/-};*Meis2*^{fl/fl} embryos stained with anti-Prep antibody, and nuclei counterstained with DAPI. *Meis1/Meis2* double mutants

did not show changes in Prep expression. nr-neural retina, lpi – lens pit. (TIF)

S1 Table. Oligonucleotides.
(DOCX)

S2 Table. Primary antibodies.
(DOCX)

Acknowledgments

We are grateful to Dr. A. Cvekl for continuous stimulating discussions during the course of this project. We express our special thanks to Dr. R. Sedlacek and Dr. I. M. Beck from the Transgenic and Archiving Module, the Czech Centre for Phenogenomics (CCP), IMG Prague for their excellent effort in generation of SIMO and EE knockout model. We would like to thank V. Noskova, A. Zitova and J. Pohorela for excellent technical assistance and Dr. A. Bruce for proofreading the manuscript. We thank F. Weisz and P. Kasperek for help and advice during preparation of TALEN constructs. We thank Drs. N. Copeland, J. Favor, A. Buchberg, P. Bovolenta, P. Carlsson, H. Kondoh, S. Ziegler, D. Kleinjan, W.Chen, and K. Kawakami for mice and reagents.

Author Contributions

Conceived and designed the experiments: ZK BA LK.

Performed the experiments: BA JS LK JL MB IK ZK.

Analyzed the data: BA LK IK ZK.

Contributed reagents/materials/analysis tools: BA OM ZK.

Wrote the paper: ZK BA LK OM.

References

1. Cvekl A, Ashery-Padan R. The cellular and molecular mechanisms of vertebrate lens development. *Development*. 2014; 141(23):4432–47. PubMed Central PMCID: PMC4302924. doi: [10.1242/dev.107953](https://doi.org/10.1242/dev.107953) PMID: [25406393](https://pubmed.ncbi.nlm.nih.gov/25406393/)
2. Gunhaga L. The lens: a classical model of embryonic induction providing new insights into cell determination in early development. *Philosophical transactions of the Royal Society of London Series B, Biological sciences*. 2011; 366(1568):1193–203. PubMed Central PMCID: PMC3061103. doi: [10.1098/rstb.2010.0175](https://doi.org/10.1098/rstb.2010.0175) PMID: [21402580](https://pubmed.ncbi.nlm.nih.gov/21402580/)
3. Bailey AP, Bhattacharyya S, Bronner-Fraser M, Streit A. Lens specification is the ground state of all sensory placodes, from which FGF promotes olfactory identity. *Developmental cell*. 2006; 11(4):505–17. doi: [10.1016/j.devcel.2006.08.009](https://doi.org/10.1016/j.devcel.2006.08.009) PMID: [17011490](https://pubmed.ncbi.nlm.nih.gov/17011490/)
4. Hill RE, Favor J, Hogan BL, Ton CC, Saunders GF, Hanson IM, et al. Mouse small eye results from mutations in a paired-like homeobox-containing gene. *Nature*. 1991; 354(6354):522–5. doi: [10.1038/354522a0](https://doi.org/10.1038/354522a0) PMID: [1684639](https://pubmed.ncbi.nlm.nih.gov/1684639/)
5. Hogan BL, Horsburgh G, Cohen J, Hetherington CM, Fisher G, Lyon MF. Small eyes (Sey): a homozygous lethal mutation on chromosome 2 which affects the differentiation of both lens and nasal placodes in the mouse. *Journal of embryology and experimental morphology*. 1986; 97:95–110. PMID: [3794606](https://pubmed.ncbi.nlm.nih.gov/3794606/)
6. Hogan BL, Hirst EM, Horsburgh G, Hetherington CM. Small eye (Sey): a mouse model for the genetic analysis of craniofacial abnormalities. *Development*. 1988; 103 Suppl:115–9. PMID: [3250848](https://pubmed.ncbi.nlm.nih.gov/3250848/)
7. Ashery-Padan R, Marquardt T, Zhou X, Gruss P. Pax6 activity in the lens primordium is required for lens formation and for correct placement of a single retina in the eye. *Genes Dev*. 2000; 14(21):2701–11. Epub 2000/11/09. PMID: [11069887](https://pubmed.ncbi.nlm.nih.gov/11069887/)

8. Collinson JM, Hill RE, West JD. Different roles for Pax6 in the optic vesicle and facial epithelium mediate early morphogenesis of the murine eye. *Development*. 2000; 127(5):945–56. PMID: [10662634](#)
9. Quinn JC, West JD, Hill RE. Multiple functions for Pax6 in mouse eye and nasal development. *Genes Dev*. 1996; 10(4):435–46. PMID: [8600027](#)
10. Matsushima D, Heavner W, Pevny LH. Combinatorial regulation of optic cup progenitor cell fate by SOX2 and PAX6. *Development*. 2011; 138(3):443–54. PubMed Central PMCID: PMC3014633. doi: [10.1242/dev.055178](#) PMID: [21205789](#)
11. Lagutin OV, Zhu CC, Kobayashi D, Topczewski J, Shimamura K, Puelles L, et al. Six3 repression of Wnt signaling in the anterior neuroectoderm is essential for vertebrate forebrain development. *Genes Dev*. 2003; 17(3):368–79. PubMed Central PMCID: PMC195989. doi: [10.1101/gad.1059403](#) PMID: [12569128](#)
12. Langer L, Taranova O, Sulik K, Pevny L. SOX2 hypomorphism disrupts development of the prechordal floor and optic cup. *Mechanisms of development*. 2012; 129(1–4):1–12. PubMed Central PMCID: PMC4077342. doi: [10.1016/j.mod.2012.04.001](#) PMID: [22522080](#)
13. Bhatia S, Monahan J, Ravi V, Gautier P, Murdoch E, Brenner S, et al. A survey of ancient conserved non-coding elements in the PAX6 locus reveals a landscape of interdigitated cis-regulatory archipelagos. *Developmental biology*. 2014; 387(2):214–28. doi: [10.1016/j.ydbio.2014.01.007](#) PMID: [24440152](#)
14. Kleinjan DA, van Heyningen V. Long-range control of gene expression: emerging mechanisms and disruption in disease. *American journal of human genetics*. 2005; 76(1):8–32. PubMed Central PMCID: PMC1196435. doi: [10.1086/426833](#) PMID: [15549674](#)
15. Kammandel B, Chowdhury K, Stoykova A, Aparicio S, Brenner S, Gruss P. Distinct cis-essential modules direct the time-space pattern of the Pax6 gene activity. *Developmental biology*. 1999; 205(1):79–97. doi: [10.1006/dbio.1998.9128](#) PMID: [9882499](#)
16. Williams SC, Altmann CR, Chow RL, Hemmati-Brivanlou A, Lang RA. A highly conserved lens transcriptional control element from the Pax-6 gene. *Mechanisms of development*. 1998; 73(2):225–9. PMID: [9622640](#)
17. Dimanlig PV, Faber SC, Auerbach W, Makarenkova HP, Lang RA. The upstream ectoderm enhancer in Pax6 has an important role in lens induction. *Development*. 2001; 128(22):4415–24. PMID: [11714668](#)
18. Fantès J, Redeker B, Breen M, Boyle S, Brown J, Fletcher J, et al. Aniridia-associated cytogenetic rearrangements suggest that a position effect may cause the mutant phenotype. *Human molecular genetics*. 1995; 4(3):415–22. PMID: [7795596](#)
19. Bhatia S, Bengani H, Fish M, Brown A, Divizia MT, de Marco R, et al. Disruption of autoregulatory feedback by a mutation in a remote, ultraconserved PAX6 enhancer causes aniridia. *American journal of human genetics*. 2013; 93(6):1126–34. PubMed Central PMCID: PMC3852925. doi: [10.1016/j.ajhg.2013.10.028](#) PMID: [24290376](#)
20. Kleinjan DA, Seawright A, Schedl A, Quinlan RA, Danes S, van Heyningen V. Aniridia-associated translocations, DNase hypersensitivity, sequence comparison and transgenic analysis redefine the functional domain of PAX6. *Human molecular genetics*. 2001; 10(19):2049–59. PMID: [11590122](#)
21. Aota S, Nakajima N, Sakamoto R, Watanabe S, Ibaraki N, Okazaki K. Pax6 autoregulation mediated by direct interaction of Pax6 protein with the head surface ectoderm-specific enhancer of the mouse Pax6 gene. *Developmental biology*. 2003; 257(1):1–13. PMID: [12710953](#)
22. Zhang X, Friedman A, Heaney S, Purcell P, Maas RL. Meis homeoproteins directly regulate Pax6 during vertebrate lens morphogenesis. *Genes Dev*. 2002; 16(16):2097–107. PubMed Central PMCID: PMC186446. doi: [10.1101/gad.1007602](#) PMID: [12183364](#)
23. Liu W, Lagutin OV, Mende M, Streit A, Oliver G. Six3 activation of Pax6 expression is essential for mammalian lens induction and specification. *The EMBO journal*. 2006; 25(22):5383–95. PubMed Central PMCID: PMC1636621. doi: [10.1038/sj.emboj.7601398](#) PMID: [17066077](#)
24. Donner AL, Episkopou V, Maas RL. Sox2 and Pou2f1 interact to control lens and olfactory placode development. *Developmental biology*. 2007; 303(2):784–99. PubMed Central PMCID: PMC3276313. doi: [10.1016/j.ydbio.2006.10.047](#) PMID: [17140559](#)
25. Rowan S, Siggers T, Lachke SA, Yue Y, Bulyk ML, Maas RL. Precise temporal control of the eye regulatory gene Pax6 via enhancer-binding site affinity. *Genes Dev*. 2010; 24(10):980–5. PubMed Central PMCID: PMC2867212. doi: [10.1101/gad.1890410](#) PMID: [20413611](#)
26. Longobardi E, Penkov D, Mateos D, De Florian G, Torres M, Blasi F. Biochemistry of the tale transcription factors PREP, MEIS, and PBX in vertebrates. *Developmental dynamics: an official publication of the American Association of Anatomists*. 2014; 243(1):59–75. PubMed Central PMCID: PMC4232920.
27. Penkov D, Mateos San Martin D, Fernandez-Diaz LC, Rossello CA, Torroja C, Sanchez-Cabo F, et al. Analysis of the DNA-binding profile and function of TALE homeoproteins reveals their specialization

- and specific interactions with Hox genes/proteins. *Cell reports*. 2013; 3(4):1321–33. doi: [10.1016/j.celrep.2013.03.029](https://doi.org/10.1016/j.celrep.2013.03.029) PMID: [23602564](https://pubmed.ncbi.nlm.nih.gov/23602564/)
28. Hisa T, Spence SE, Rachel RA, Fujita M, Nakamura T, Ward JM, et al. Hematopoietic, angiogenic and eye defects in Meis1 mutant animals. *The EMBO journal*. 2004; 23(2):450–9. PubMed Central PMCID: PMC1271748. doi: [10.1038/sj.emboj.7600038](https://doi.org/10.1038/sj.emboj.7600038) PMID: [14713950](https://pubmed.ncbi.nlm.nih.gov/14713950/)
 29. Swift GH, Liu Y, Rose SD, Bischof LJ, Steelman S, Buchberg AM, et al. An endocrine-exocrine switch in the activity of the pancreatic homeodomain protein PDX1 through formation of a trimeric complex with PBX1b and MRG1 (MEIS2). *Molecular and cellular biology*. 1998; 18(9):5109–20. PubMed Central PMCID: PMC109096. PMID: [9710595](https://pubmed.ncbi.nlm.nih.gov/9710595/)
 30. Toresson H, Parmar M, Campbell K. Expression of Meis and Pbx genes and their protein products in the developing telencephalon: implications for regional differentiation. *Mechanisms of development*. 2000; 94(1–2):183–7. PMID: [10842069](https://pubmed.ncbi.nlm.nih.gov/10842069/)
 31. Grindley JC, Davidson DR, Hill RE. The role of Pax-6 in eye and nasal development. *Development*. 1995; 121(5):1433–42. PMID: [7789273](https://pubmed.ncbi.nlm.nih.gov/7789273/)
 32. Machon O, Masek J, Machonova O, Krauss S, Kozmik Z. Meis2 is essential for cranial and cardiac neural crest development. *BMC developmental biology*. 2015; 15:40. PubMed Central PMCID: PMC4636814. doi: [10.1186/s12861-015-0093-6](https://doi.org/10.1186/s12861-015-0093-6) PMID: [26545946](https://pubmed.ncbi.nlm.nih.gov/26545946/)
 33. Blixt A, Landgren H, Johansson BR, Carlsson P. Foxe3 is required for morphogenesis and differentiation of the anterior segment of the eye and is sensitive to Pax6 gene dosage. *Developmental biology*. 2007; 302(1):218–29. doi: [10.1016/j.ydbio.2006.09.021](https://doi.org/10.1016/j.ydbio.2006.09.021) PMID: [17064680](https://pubmed.ncbi.nlm.nih.gov/17064680/)
 34. Smith AN, Miller LA, Radice G, Ashery-Padan R, Lang RA. Stage-dependent modes of Pax6-Sox2 epistasis regulate lens development and eye morphogenesis. *Development*. 2009; 136(17):2977–85. PubMed Central PMCID: PMC2723069. doi: [10.1242/dev.037341](https://doi.org/10.1242/dev.037341) PMID: [19666824](https://pubmed.ncbi.nlm.nih.gov/19666824/)
 35. Purcell P, Oliver G, Mardon G, Donner AL, Maas RL. Pax6-dependence of Six3, Eya1 and Dach1 expression during lens and nasal placode induction. *Gene expression patterns: GEP*. 2005; 6(1):110–8. doi: [10.1016/j.modgep.2005.04.010](https://doi.org/10.1016/j.modgep.2005.04.010) PMID: [16024294](https://pubmed.ncbi.nlm.nih.gov/16024294/)
 36. Chang CP, Jacobs Y, Nakamura T, Jenkins NA, Copeland NG, Cleary ML. Meis proteins are major in vivo DNA binding partners for wild-type but not chimeric Pbx proteins. *Molecular and cellular biology*. 1997; 17(10):5679–87. PubMed Central PMCID: PMC232416. PMID: [9315626](https://pubmed.ncbi.nlm.nih.gov/9315626/)
 37. Yamada T, Nakamura T, Westphal H, Russell P. Synthesis of alpha-crystallin by a cell line derived from the lens of a transgenic animal. *Current eye research*. 1990; 9(1):31–7. PMID: [2178867](https://pubmed.ncbi.nlm.nih.gov/2178867/)
 38. Zhang X, Rowan S, Yue Y, Heaney S, Pan Y, Brendolan A, et al. Pax6 is regulated by Meis and Pbx homeoproteins during pancreatic development. *Developmental biology*. 2006; 300(2):748–57. doi: [10.1016/j.ydbio.2006.06.030](https://doi.org/10.1016/j.ydbio.2006.06.030) PMID: [17049510](https://pubmed.ncbi.nlm.nih.gov/17049510/)
 39. Farley EK, Olson KM, Zhang W, Brandt AJ, Rokhsar DS, Levine MS. Suboptimization of developmental enhancers. *Science*. 2015; 350(6258):325–8. PubMed Central PMCID: PMC4970741. doi: [10.1126/science.aac6948](https://doi.org/10.1126/science.aac6948) PMID: [26472909](https://pubmed.ncbi.nlm.nih.gov/26472909/)
 40. Bessa J, Tena JJ, de la Calle-Mustienes E, Fernandez-Minan A, Naranjo S, Fernandez A, et al. Zebrafish enhancer detection (ZED) vector: a new tool to facilitate transgenesis and the functional analysis of cis-regulatory regions in zebrafish. *Developmental dynamics: an official publication of the American Association of Anatomists*. 2009; 238(9):2409–17.
 41. Davidson EH. Emerging properties of animal gene regulatory networks. *Nature*. 2010; 468(7326):911–20. PubMed Central PMCID: PMC3967874. doi: [10.1038/nature09645](https://doi.org/10.1038/nature09645) PMID: [21164479](https://pubmed.ncbi.nlm.nih.gov/21164479/)
 42. Davidson EH, Levine MS. Properties of developmental gene regulatory networks. *Proceedings of the National Academy of Sciences of the United States of America*. 2008; 105(51):20063–6. PubMed Central PMCID: PMC2629280. doi: [10.1073/pnas.0806007105](https://doi.org/10.1073/pnas.0806007105) PMID: [19104053](https://pubmed.ncbi.nlm.nih.gov/19104053/)
 43. Goudreau G, Petrou P, Reneker LW, Graw J, Loster J, Gruss P. Mutually regulated expression of Pax6 and Six3 and its implications for the Pax6 haploinsufficient lens phenotype. *Proceedings of the National Academy of Sciences of the United States of America*. 2002; 99(13):8719–24. PubMed Central PMCID: PMC124365. doi: [10.1073/pnas.132195699](https://doi.org/10.1073/pnas.132195699) PMID: [12072567](https://pubmed.ncbi.nlm.nih.gov/12072567/)
 44. Lang RA. Pathways regulating lens induction in the mouse. *The International journal of developmental biology*. 2004; 48(8–9):783–91. doi: [10.1387/ijdb.041903rf](https://doi.org/10.1387/ijdb.041903rf) PMID: [15558471](https://pubmed.ncbi.nlm.nih.gov/15558471/)
 45. Carbe C, Hertzler-Schaefer K, Zhang X. The functional role of the Meis/Prep-binding elements in Pax6 locus during pancreas and eye development. *Developmental biology*. 2012; 363(1):320–9. PubMed Central PMCID: PMC3288747. doi: [10.1016/j.ydbio.2011.12.038](https://doi.org/10.1016/j.ydbio.2011.12.038) PMID: [22240097](https://pubmed.ncbi.nlm.nih.gov/22240097/)
 46. Marcos S, Gonzalez-Lazaro M, Beccari L, Carramolino L, Martin-Bermejo MJ, Amarie O, et al. Meis1 coordinates a network of genes implicated in eye development and microphthalmia. *Development*. 2015; 142(17):3009–20. doi: [10.1242/dev.122176](https://doi.org/10.1242/dev.122176) PMID: [26253404](https://pubmed.ncbi.nlm.nih.gov/26253404/)

47. Jordan T, Hanson I, Zaletayev D, Hodgson S, Prosser J, Seawright A, et al. The human PAX6 gene is mutated in two patients with aniridia. *Nature genetics*. 1992; 1(5):328–32. doi: [10.1038/ng0892-328](https://doi.org/10.1038/ng0892-328) PMID: [1302030](https://pubmed.ncbi.nlm.nih.gov/1302030/)
48. Ton CC, Hirvonen H, Miwa H, Weil MM, Monaghan P, Jordan T, et al. Positional cloning and characterization of a paired box- and homeobox-containing gene from the aniridia region. *Cell*. 1991; 67(6):1059–74. PMID: [1684738](https://pubmed.ncbi.nlm.nih.gov/1684738/)
49. Glaser T, Walton DS, Maas RL. Genomic structure, evolutionary conservation and aniridia mutations in the human PAX6 gene. *Nature genetics*. 1992; 2(3):232–9. doi: [10.1038/ng1192-232](https://doi.org/10.1038/ng1192-232) PMID: [1345175](https://pubmed.ncbi.nlm.nih.gov/1345175/)
50. Kroeber M, Davis N, Holzmann S, Kritzenberger M, Shelah-Goraly M, Ofri R, et al. Reduced expression of Pax6 in lens and cornea of mutant mice leads to failure of chamber angle development and juvenile glaucoma. *Human molecular genetics*. 2010; 19(17):3332–42. doi: [10.1093/hmg/ddq237](https://doi.org/10.1093/hmg/ddq237) PMID: [20538882](https://pubmed.ncbi.nlm.nih.gov/20538882/)
51. Schedl A, Ross A, Lee M, Engelkamp D, Rashbass P, van Heyningen V, et al. Influence of PAX6 gene dosage on development: overexpression causes severe eye abnormalities. *Cell*. 1996; 86(1):71–82. PMID: [8689689](https://pubmed.ncbi.nlm.nih.gov/8689689/)
52. Shaham O, Smith AN, Robinson ML, Taketo MM, Lang RA, Ashery-Padan R. Pax6 is essential for lens fiber cell differentiation. *Development*. 2009; 136(15):2567–78. PubMed Central PMCID: [PMC2709063](https://pubmed.ncbi.nlm.nih.gov/PMC2709063/). doi: [10.1242/dev.032888](https://doi.org/10.1242/dev.032888) PMID: [19570848](https://pubmed.ncbi.nlm.nih.gov/19570848/)
53. Hong JW, Hendrix DA, Levine MS. Shadow enhancers as a source of evolutionary novelty. *Science*. 2008; 321(5894):1314. PubMed Central PMCID: [PMC4257485](https://pubmed.ncbi.nlm.nih.gov/PMC4257485/). doi: [10.1126/science.1160631](https://doi.org/10.1126/science.1160631) PMID: [18772429](https://pubmed.ncbi.nlm.nih.gov/18772429/)
54. Carroll SB. Evo-devo and an expanding evolutionary synthesis: a genetic theory of morphological evolution. *Cell*. 2008; 134(1):25–36. doi: [10.1016/j.cell.2008.06.030](https://doi.org/10.1016/j.cell.2008.06.030) PMID: [18614008](https://pubmed.ncbi.nlm.nih.gov/18614008/)
55. Prud'homme B, Gompel N, Carroll SB. Emerging principles of regulatory evolution. *Proceedings of the National Academy of Sciences of the United States of America*. 2007; 104 Suppl 1:8605–12. PubMed Central PMCID: [PMC1876436](https://pubmed.ncbi.nlm.nih.gov/PMC1876436/).
56. Frankel N, Davis GK, Vargas D, Wang S, Payre F, Stern DL. Phenotypic robustness conferred by apparently redundant transcriptional enhancers. *Nature*. 2010; 466(7305):490–3. PubMed Central PMCID: [PMC2909378](https://pubmed.ncbi.nlm.nih.gov/PMC2909378/). doi: [10.1038/nature09158](https://doi.org/10.1038/nature09158) PMID: [20512118](https://pubmed.ncbi.nlm.nih.gov/20512118/)
57. Perry MW, Boettiger AN, Bothma JP, Levine M. Shadow enhancers foster robustness of *Drosophila* gastrulation. *Current biology: CB*. 2010; 20(17):1562–7. PubMed Central PMCID: [PMC4257487](https://pubmed.ncbi.nlm.nih.gov/PMC4257487/). doi: [10.1016/j.cub.2010.07.043](https://doi.org/10.1016/j.cub.2010.07.043) PMID: [20797865](https://pubmed.ncbi.nlm.nih.gov/20797865/)
58. Perry MW, Bothma JP, Luu RD, Levine M. Precision of hunchback expression in the *Drosophila* embryo. *Current biology: CB*. 2012; 22(23):2247–52. PubMed Central PMCID: [PMC4257490](https://pubmed.ncbi.nlm.nih.gov/PMC4257490/). doi: [10.1016/j.cub.2012.09.051](https://doi.org/10.1016/j.cub.2012.09.051) PMID: [23122844](https://pubmed.ncbi.nlm.nih.gov/23122844/)
59. Ghiasvand NM, Rudolph DD, Mashayekhi M, Brzezinski JAt, Goldman D, Glaser T. Deletion of a remote enhancer near ATOH7 disrupts retinal neurogenesis, causing NCRNA disease. *Nature neuroscience*. 2011; 14(5):578–86. PubMed Central PMCID: [PMC3083485](https://pubmed.ncbi.nlm.nih.gov/PMC3083485/). doi: [10.1038/nn.2798](https://doi.org/10.1038/nn.2798) PMID: [21441919](https://pubmed.ncbi.nlm.nih.gov/21441919/)
60. Cannavo E, Khoueiry P, Garfield DA, Geeleher P, Zichner T, Gustafson EH, et al. Shadow Enhancers Are Pervasive Features of Developmental Regulatory Networks. *Current biology: CB*. 2016; 26(1):38–51. PubMed Central PMCID: [PMC4712172](https://pubmed.ncbi.nlm.nih.gov/PMC4712172/). doi: [10.1016/j.cub.2015.11.034](https://doi.org/10.1016/j.cub.2015.11.034) PMID: [26687625](https://pubmed.ncbi.nlm.nih.gov/26687625/)
61. Ravi V, Bhatia S, Gautier P, Loosli F, Tay BH, Tay A, et al. Sequencing of Pax6 loci from the elephant shark reveals a family of Pax6 genes in vertebrate genomes, forged by ancient duplications and divergences. *PLoS genetics*. 2013; 9(1):e1003177. PubMed Central PMCID: [PMC3554528](https://pubmed.ncbi.nlm.nih.gov/PMC3554528/). doi: [10.1371/journal.pgen.1003177](https://doi.org/10.1371/journal.pgen.1003177) PMID: [23359656](https://pubmed.ncbi.nlm.nih.gov/23359656/)
62. Gehring WJ, Ikeo K. Pax 6: mastering eye morphogenesis and eye evolution. *Trends in genetics: TIG*. 1999; 15(9):371–7. PMID: [10461206](https://pubmed.ncbi.nlm.nih.gov/10461206/)
63. Mukherjee K, Burglin TR. Comprehensive analysis of animal TALE homeobox genes: new conserved motifs and cases of accelerated evolution. *Journal of molecular evolution*. 2007; 65(2):137–53. doi: [10.1007/s00239-006-0023-0](https://doi.org/10.1007/s00239-006-0023-0) PMID: [17665086](https://pubmed.ncbi.nlm.nih.gov/17665086/)
64. Pai CY, Kuo TS, Jaw TJ, Kurant E, Chen CT, Bessarab DA, et al. The Homothorax homeoprotein activates the nuclear localization of another homeoprotein, extradenticle, and suppresses eye development in *Drosophila*. *Genes Dev*. 1998; 12(3):435–46. PubMed Central PMCID: [PMC316489](https://pubmed.ncbi.nlm.nih.gov/PMC316489/). PMID: [9450936](https://pubmed.ncbi.nlm.nih.gov/9450936/)
65. Wang CW, Sun YH. Segregation of eye and antenna fates maintained by mutual antagonism in *Drosophila*. *Development*. 2012; 139(18):3413–21. doi: [10.1242/dev.078857](https://doi.org/10.1242/dev.078857) PMID: [22912416](https://pubmed.ncbi.nlm.nih.gov/22912416/)
66. Soriano P. Generalized lacZ expression with the ROSA26 Cre reporter strain. *Nature genetics*. 1999; 21(1):70–1. doi: [10.1038/5007](https://doi.org/10.1038/5007) PMID: [9916792](https://pubmed.ncbi.nlm.nih.gov/9916792/)

67. Cermak T, Doyle EL, Christian M, Wang L, Zhang Y, Schmidt C, et al. Efficient design and assembly of custom TALEN and other TAL effector-based constructs for DNA targeting. *Nucleic acids research*. 2011; 39(12):e82. PubMed Central PMCID: PMC3130291. doi: [10.1093/nar/gkr218](https://doi.org/10.1093/nar/gkr218) PMID: [21493687](https://pubmed.ncbi.nlm.nih.gov/21493687/)
68. Kasperek P, Krausova M, Haneckova R, Kriz V, Zbodakova O, Korinek V, et al. Efficient gene targeting of the *Rosa26* locus in mouse zygotes using TALE nucleases. *FEBS letters*. 2014; 588(21):3982–8. doi: [10.1016/j.febslet.2014.09.014](https://doi.org/10.1016/j.febslet.2014.09.014) PMID: [25241166](https://pubmed.ncbi.nlm.nih.gov/25241166/)
69. Machon O, Kreslova J, Ruzickova J, Vacik T, Klimova L, Fujimura N, et al. Lens morphogenesis is dependent on Pax6-mediated inhibition of the canonical Wnt/beta-catenin signaling in the lens surface ectoderm. *Genesis*. 2010; 48(2):86–95. doi: [10.1002/dvg.20583](https://doi.org/10.1002/dvg.20583) PMID: [20027618](https://pubmed.ncbi.nlm.nih.gov/20027618/)
70. Sandelin A, Alkema W, Engstrom P, Wasserman WW, Lenhard B. JASPAR: an open-access database for eukaryotic transcription factor binding profiles. *Nucleic acids research*. 2004; 32(Database issue): D91–4. PubMed Central PMCID: PMC308747. doi: [10.1093/nar/gkh012](https://doi.org/10.1093/nar/gkh012) PMID: [14681366](https://pubmed.ncbi.nlm.nih.gov/14681366/)
71. Starostova M, Cermak V, Dvorakova M, Karafiat V, Kosla J, Dvorak M. The oncoprotein v-Myb activates transcription of Gremlin 2 during in vitro differentiation of the chicken neural crest to melanoblasts. *Gene*. 2014; 540(1):122–9. doi: [10.1016/j.gene.2014.02.031](https://doi.org/10.1016/j.gene.2014.02.031) PMID: [24576577](https://pubmed.ncbi.nlm.nih.gov/24576577/)
72. Kawakami K, Takeda H, Kawakami N, Kobayashi M, Matsuda N, Mishina M. A transposon-mediated gene trap approach identifies developmentally regulated genes in zebrafish. *Developmental cell*. 2004; 7(1):133–44. doi: [10.1016/j.devcel.2004.06.005](https://doi.org/10.1016/j.devcel.2004.06.005) PMID: [15239961](https://pubmed.ncbi.nlm.nih.gov/15239961/)